Ref. Ares(2026)2334111 - 03/03/2026

D8.2: Life Cycle Evaluation Report

COCOLIH2T

Composite Conformal Liquid H_2 Tank

Project information

Project Acronym	COCOLIH2T
Project Full Title	Composite Conformal Liquid H_2 Tank
Grant Agreement	101101404
Project Duration	36 months
Project Coordinator	COLLINS

Deliverable information

Deliverable Title	D8.2 – Life cycle evaluation report
Deliverable nature	R (Report)
Dissemination Level	PU (Public)
Due date	31/01/2026
Submission date	30/01/2026
Deliverable Leader	John-Alan Pascoe TUD
Deliverable Contributors	Nikhil Garg TUD, Mirko Simonetto TUD
Reviewers	Paul Liddel SAFRAN, Kostas Kouramas COLLINS, Jack Cullinan COLLINS,

Clean Hydrogen Partnership   Co-funded by the European Union

The project is supported by the Clean Hydrogen Partnership and its members. Views and opinions expressed are however those of the author(s) only and do not necessarily reflect those of the European Union or Clean Hydrogen Joint Undertaking. Neither the European Union nor the granting authority can be held responsible for them. This document has been produced under Grant Agreement 101101404.

Revision history

Issue	Date	Comment	Author
V0.1	30/01/2026	Initial draft	Nikhil Garg (TUD), Mirko Simonetto (TUD)
V1.0	30/01/2026	Final draft	Jack Cullinan (Collins, Coordinator)

Table of Contents

List of Abbreviations

Abbreviation	Meaning
AFP	Automated Fibre Placement
AI	Artificial Intelligence
CF	Carbon Fibre
CFRP	Carbon Fibre Reinforced Polymer
COPV	Composite Overwrapped Pressure Vessel
CT	Computed Tomography
EAF	Electric Arc Furnace
EoL	End of Life
FRP	Fibre Reinforced Polymer
FW	Filament Winding
LCA	Life Cycle Assessment
MDF	Medium Density Fibreboard
PAEK	Poly-aryl-ether-ketone
PEEK	Poly-ether-ether-ketone
PU	Poly-urethane

List of Tables

List of Figures

1 Executive Summary

The aim of the COCOLIH2T project is to contribute to the transition to hydrogen as an energy carrier in the aviation sector, by developing a conformal composite liquid hydrogen tank. While transitioning to hydrogen can mitigate greenhouse gas (GHG) emissions during operations, it is important to understand the overall impact on sustainability of the solutions developed, beyond just the GHG emissions during use. This report presents the work done in the COCOLIH2T project to understand the durability and life cycle impact (LCI) characteristics of the developed liquid hydrogen tank design.

As a full material fatigue characterisation campaign was out of scope for COCOLIH2T, the durability analysis focused on matrix crack evolution under static loading. A model was developed based on discounting the permeation barrier properties of cracked plies. This enables evaluating the hydrogen leakage rate at the tank level, as a result of a given internal (over)pressure. This also enables identification of hot-spots for future fatigue analysis.

The analysis indicated that for the tank as designed, no loss of hydrogen barrier performance due to matrix cracking would occur below the maximum operating pressure.

Life cycle analysis (LCA) focused on understanding of the impact of the COCOLIH2T design, making use of thermoplastic resin and automated fibre placement (AFP), when compared to a baseline case using thermoset resin and filament winding. Due to the aforementioned limitations on fatigue modelling the expected fatigue life of the tank could not be calculated and thus the LCA focused on the impacts during manufacturing and end-of-life (EoL).

The LCA revealed a strong dependence on various assumptions, e.g. the service life of required molds and mandrels. If the impact due to molds and mandrels is spread over 100 tanks, the increased inner tank material usage and increased energy intensity of AFP leads to an increased environmental impact for the COCOLIH2T design across all impact indicators investigated. This impact can be mitigated by ensuring recycling of the tank after EoL. It should also be noted here, that this analysis did not consider any potential environmental credits during the use-phase (i.e. aircraft operation), which should be investigated in a future analysis at the level of the entire aircraft or air transport system.

2 Introduction

While the focus on hydrogen aviation research is on eliminating the greenhouse gas emissions caused by aircraft propulsion, other aspects of sustainability should not be neglected. Within the COCOLIH2T project, the main objective is to contribute to the development of liquid hydrogen storage systems suitable for use onboard aircraft. Such systems are of course crucial in enabling the transition towards carbon-neutral fuels.

However, to optimise the design of a hydrogen storage system it is important to understand the expected lifetime of the design, as well as its life cycle impact (LCI) across a broad range of sustainability indicators. Ideally, target service life and LCI should already be considered in the system design phase. However, given the limitations of the state of the art at the start of the project and the ambitious timeline, it was already foreseen that including these aspects in the design would not be feasible for the COCOLIH2T demonstrators. Instead, it was decided to perform parallel activities to understand the expected durability and LCI characteristics of the developed demonstrator, in order to provide lessons learned, recommendations for improvement (where applicable) and contribute to a route to technology readiness level (TRL) 9.

This work was split into two parts, which are presented separately in this report. The first part focused on understanding the durability of the COCOLIH2T design solution. The state of the art proved insufficient to support developing a fatigue model, as this would require a materials testing campaign that was beyond the scope of COCOLIH2T. Instead, while some preliminary fatigue tests were performed, work focused on developing the capability to model matrix crack evolution and the consequent leak rate at tank level. Additionally, this modelling capability was used to analyse the damage detection capability of the fibre Bragg grating (FBG) sensor systems developed in WP6. Since it proved to be infeasible to provide a predicted fatigue life for the tank, the expected service life of the tank could not be provided as input for the life cycle analysis (LCA), and the two parts of the work were not connected.

The second part of the work described in this report is the LCA of the COCOLIH2T design. Of particular interest were to understand the impact of selecting a thermoplastic resin-based conformal tank, manufactured by automated fibre placement (AFP), compared to the more traditional filament wound thermoset resin-based solution, which was used as a baseline. As noted above, the expected service life of the tank (based on a fatigue and damage tolerance evaluation) could not be provided and thus the use-phase was not investigated. Instead, the LCA focused on understanding the impact during the manufacturing and end-of-life (EoL) phases of the COCOLI2T design, as compared to a baseline solution.

Both parts of this work are presented sequentially in this report.

Part I: Matrix Cracking and Durability

3 Damage tolerance evaluation of composite conformal tanks

This chapter introduces the degradation phenomena of composite laminates and the consequent required evaluations that must be performed in order to design and ensure a safe service life for a liquid hydrogen storage system vessel manufactured with this material.

3.1 Liquid hydrogen storage systems for aviation

The relevance of liquid hydrogen storage systems for aviation applications revolves around their gravimetric efficiency and dormancy limits. As the volume of the fuel increases significantly when switching from conventional jet fuel, high performance light materials are evaluated for the enveloping structure. Recent publicly available evaluations [1] reports the potential of certain aluminium alloys and composite laminates, while pointing the lack of relevant fatigue characterization in the latter case. This section introduces the system itself with the aim to understand the evaluations that must be conducted during the design and service of the cryogenic storage system.

3.1.1 System definition and applicable requirements

The liquid hydrogen (LH_2) storage tank is fundamentally a cryogenic pressure vessel designed to contain hydrogen in its liquid phase at extremely low temperatures while maintaining a controlled internal pressure. The system needs to incorporate a thermally insulated configuration to limit heat ingress and thereby manage boil-off. The solution chosen in COCOLIH2T and found in many other tank designs is a double walled tank with vacuum insulation, supported by multi-layer insulation (MLI) blankets to prevent heat transfer by radiation. Unlike conventional fuel tanks, the LH_2 tank must actively control vapor generation and discharge through a managed venting and pressure control architecture. Loss of insulation or degradation of cooling performance represents a primary design driver, as either condition can rapidly increase boil-off rates and internal pressure. Consequently, the tank and associated systems must be designed to tolerate off-nominal thermal conditions without loss of containment or uncontrolled hydrogen release.

From a systems perspective, the LH_2 tank shares baseline characteristics with other aerospace pressure vessels: it must withstand defined limit and ultimate loads, integrate into primary airframe structure with positive load paths, maintain structural integrity under emergency landing conditions, and remain retained without detachment during crash scenarios. As with other hazardous-energy storage systems, safety zoning, vent routing, over-pressure protection, and failure management are core requirements. However, the aircraft LH_2 cryotank is not directly equivalent to conventional fuel tanks, high-pressure gas cylinders, or marine cryogenic tanks, and those taxonomies should not be used. IMO/IGC "Type C" tanks are shipboard, code-defined, pressurized independent tanks for maritime service. "Type 4" and "Type 5" pressure vessels refer to composite cylinders with and without polymer liner, both intended for high-pressure compressed gas storage at near-ambient temperature. An aircraft LH_2 tank, by contrast, is a vacuum-insulated Dewar-type vessel designed for low-pressure liquid hydrogen, stringent thermal isolation, and structural integration within the airframe. Shapes may range from cylindrical to toroidal or conformal geometries depending on aircraft integration constraints, further differentiating them from standardized cylindrical composite overwrapped pressure vessels (COPV)s.

Certification of large aircraft LH_2 storage will fall under EASA CS-25 and FAA 14 CFR Part 25 as a novel fuel storage system, with compliance established through Special Conditions, Issue Papers, and agreed Means of Compliance supported by analysis, test evidence, and system safety assessments in accordance with ARP4754A and ARP4761 methodologies. In addition to demonstrating pressure vessel integrity, the design must satisfy aircraft-specific structural loads, crash deceleration requirements (vertical and longitudinal), post-crash survivability, fire exposure tolerance, and prevention of catastrophic rupture leading to hydrogen release in otherwise survivable accidents. Venting system performance, ignition prevention, leakage detection, and hazard zoning must be addressed at the aircraft level, including scenarios involving hydrogen migration into occupied or equipment bays such as the passenger cabin, avionics compartments, or cargo holds.

A defining aspect of LH_2 tank design is that containment degradation modes directly drive architecture and safety features. Key risks include uncontrolled hydrogen release and accumulation resulting from long ground holds at ambient conditions, loss of vacuum insulation, pressure relief or vent valve malfunction, fire exposure, structural penetration, and impact damage. These hazards require layered mitigation: robust structural design, vacuum monitoring, pressure control redundancy, hydrogen detection, automatic isolation and ventilation actions, and crash-resistant installation. Because prescriptive regulatory standards for aircraft LH_2 tanks do not yet exist, continued airworthiness, inspectability, and in-service monitoring requirements re integral part of the system definition from the initial design.

3.1.2 Service load scenario

This section focuses on the mechanical loads acting on the composite internal tank of the cryotank system. The internal tank is supported within the outer tank by a support structure which minimizes the contact surface to reduce the conduction heat transfer. The main loads are categorized based on their source as follows:

- S1. Thermal loads
  - a. Material
  - b. Structure
  - c. Interfaces
  - d. Gradients
- S2. Pressure loads
- S3. Inertial loads
  - a. Internal sloshing
  - b. External supports
- S4. Other conditions
  - a. Accidental crashes, penetrations
  - b. Chemical exposure
  - c. Diffusion to imperfections

The laminate material, as it is composed by different plies which are in turn composed of its constituents fibre and matrix, by definition is not uniform and thus is subject to different hierarchies of loads. Source S1.a introduces thermal loading effects, specifically the development of thermal strain in the laminate when it is exposed to temperatures different from the consolidation temperature. This is one of the most significant contributing factors and it is attributed to the difference between the coefficient of thermal expansions of fibre and matrix, and thus of subsequent plies or tapes laid down with different orientations. This phenomena was introduced and is explained in more detail in Ref. [2].

Effects of type S1.b. and S1.c. are manifested from the same cause but are acting on a different scale. Within the structure of the tank itself there might be some different areas which have distinct thermal expansion. This can be as a result of different overall stacking sequences, or geometry (S1.b.), or caused by the presence of interfaces with other components, which may be manufactured with different materials compared to the rest of the tank (S1.c.). This effect can become non-significant when mitigated with a careful design, while failing to do so can result in extensive damage between those interfaces or in the surrounding areas.

The thermal gradient labelled as cause S1.d. may refer to two different scenarios; the thermal gradients that originate from the transient condition which may happen during the fuelling process of the tank, and the gradient that originates between two sections of the tank at different temperature, for example due to the fuel level or as a consequence of the temperature difference between the inner and outer side of the tank wall. The intensity of these effects depends on the defined tank operations, e.g. the temperature of the tank during the refuelling process or the methods for extracting the hydrogen from the tank itself, which in some cases may warm up the ullage, the gaseous fraction of the stored hydrogen.

The tank is pressurized to a defined level during the operations, which results in a distribution of strains within the laminate thickness (S2.), adding up with the local thermal stresses. The bi-axiality of the load depends on the local geometry and location, but as the tank converges towards convex closed surface the ratio is overall uniform. As a consequence, all layers within the laminate could potentially crack and form open leakage paths.

The inertial loads classified as sloshing (S3.a.) are defined as the impacts of the liquid fuel onto the internal surfaces of the inner tank when the fluid is moving due to external inertial adjustment. This type of load hits the surface in random locations, with a distribution that follows the physics of the liquid and the inertial loads during flight. The inertial loads on the outer surface of the inner tank (S3.b.), are instead applied on specific locations defined by the supports of the inner tank. The intensity depends on the flight loads and the design of these supports, specifically their contact interface.

Collisions of the tank with external, foreign objects must be evaluated in a broader analysis where accidental or malicious damage is expected (S4.a.), this must consider both the internal and external vessel. The exposure of materials to a hydrogen-rich environment will result in the diffusion of H atoms and H_2 molecules within the material structure, which can cause different effects depending on the material affinity. The chemical effects source (S4.b.) refer to these uniform or gradient changes in the material properties caused by hydrogen bonds or physical interaction of the hydrogen molecules fitting within the material atomic structure. The last effect source (S4.c.), refers instead to hydrogen accumulation within void pockets or material interfaces, which can result in morphological changes, material alterations, and unexpected damage when the thermodynamic conditions change (e.g. volume changes due to freezing or boiling). These types of effects are highly dependent on the material quality and its homogeneity within the structure.

3.2 Relevant material strength and durability characterization

The most relevant damage phenomenon within the context is the microcracking of the laminate layers, which leads to an interconnected network of surface openings which significantly degrades the permeation barrier, ultimately leading to leakage of hydrogen. This section analyses the phenomena of formation of these crack and the relevant characterization campaign for both static and fatigue conditions.

3.2.1 Phenomenology of the microcrack formation

The microcrack formation is one of the first manifestations of laminate degradation. These cracks are often called transverse cracks, as they run parallel to the fibres and orthogonal to the load direction, as represented in Figure 1. In the case of a pressurized tank with thermal loads, a biaxial load will allow for cracks to generate in each layer, independent from their orientation. This happened during the testing of the X-33 spaceplane [3], and a simplified post evaluation of these effects has been provided by the NASA technical reports in Ref [4] and [5], and again by Ref [6].

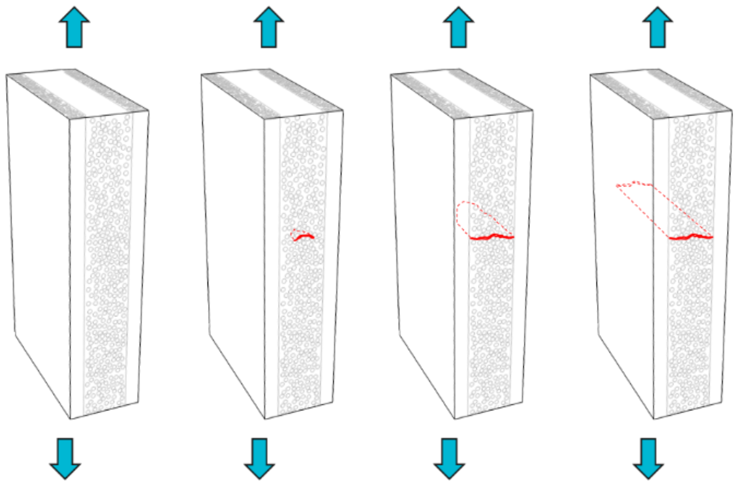

Figure 1 – Representation of the transverse crack formation process in a cross-ply laminate subject to unidirectional loading. In the first three images the propagation is mostly through the thickness, while on the fourth image the propagation is through the width, or the so-called tunnelling propagation. No delamination is represented.

To postpone the formation of transverse cracks during service conditions, and eventually just consider their formation on certain layers during the lifecycle of the tank in a damage tolerance scenario, three main actions can be applied during the material selection. First, the layer thickness should be reduced, thus reducing the strain energy available to open a crack given an initial defect or debonding within the material. Second, a matrix material with higher strength and toughness should be selected, requiring thus a higher energy to open the crack itself. Third, selecting a fibre material with a coefficient of thermal expansion closer to the matrix can reduce the amount of thermal strain, which itself is a significant part of the total load in standard carbon fibre reinforced epoxy applications in cryogenic environments.

The effect of layer thickness has been initially observed and analysed by Parvizi et al. [7], introducing the need of a fracture mechanics approach to align strength data from the same material with different thickness of the cracking layer. The amount of applicable total strain to open a crack at different temperatures can be considered to be constant, when the hypothesis that strength and toughness are not varying significantly with temperature are fulfilled. By calculating the thermal strains at room temperature, the total strain limit can be computed, as the total strain is the sum of the mechanical and thermal components. In this way, as analytically proposed by Garcia et al. [8], the room temperature limits can be translated to the application temperature.

Quasi-isotropic laminates are often preferred in structural applications, as they provide more reliable results. The characterized cracking strength of crossply plies can still be applied, by evaluating the local transverse strain ε_{22} or the stress σ_{22} of each ply. A different case applies instead when more exotic stacking sequences are employed, or also when load cases different than in-plane traction are applied. It has been demonstrated that when the in plane shear components are on the same order of magnitude as the in-plane transverse stress, a different type of damage process is observed and the formation of cracks is anticipated with respect to the evaluation based on the transverse strain/stress only [9]. This result is valid for epoxy matrix based materials but it can be expected that thermoplastics will behave similarly.

Another important aspect to introduce is the formation of the transverse cracks in fatigue conditions. Constant amplitude loading of laminates at strain levels below the coalescence limit introduced before, will produce the progressive formation and propagation of cracks distributed within the ply, as represented progressively in Figure 1. The interaction of these cracks with each other may lower the tip strain and stop the tunnelling propagation [10], while applying variable amplitude stresses can anticipate the crack formation, rendering the linear damage accumulation (Palmgren-Miner) rule unsafe for predicting this type of phenomenon [11]. Loading below the debonding limit can be the solution to avoid the formation of transverse cracks in a laminate without defects and free interfaces, but this limit has to be carefully determined for each fibre-matrix configuration. A detailed analysis of this micromechanical crack formation process has been performed for epoxy matrices in Ref. [12], while an approach for characterization and prediction of fatigue crack formation under fatigue loads is proposed in Ref. [10].

3.2.2 Characterization of microcrack strength

The critical damage in the case of liquid hydrogen containment is a network of ply extended cracks, interconnected between subsequent layer, such that the vacuum insulation is reduced to a point where the heat balance is compromised. A crack spanning a single layer is shown in Figure 2 at two stages of its development, which is usually instantaneous in the case of static load application or follows a propagation in the case of repeated load.

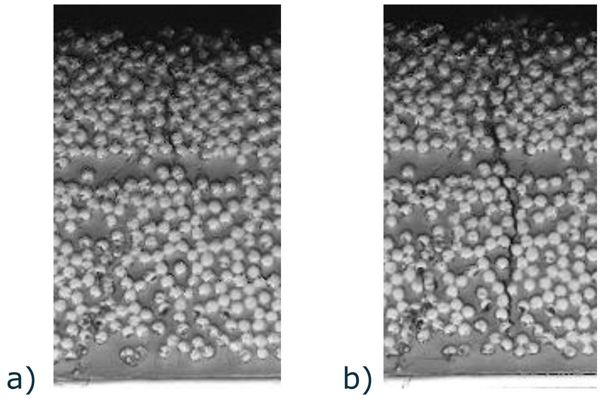

Figure 2 – Transverse crack propagation as observed on the external layer of crossply sample side subject to interrupted fatigue evaluation.

Different observation methods could be applied for characterizing this phenomenon. Sample edge observation is typically employed during the characterization of cracks on cross-ply laminates, given the often dismissible effect of free edges on stress, but it requires an accurate polishing of the edge surface to avoid premature crack formation due to the cutting machine marks, please note this happens as well for waterjet-cut samples [13]. Some sample design does not allow for edge polishing, thus the crack counting process might be performed after destructive sectioning of the sample, ruling out the edge effects when damage is limited. Other methods such as the edge replica are applied to characterize the crack formation process, or the usage of penetrant liquids together with the x-ray imaging. Transparent samples can take advantage of transmitted light observations.

As a crack is a 3D void represented by the enclosing surfaces, three main directions are mainly involved. In the context of this analysis, cracks are only counted and not evaluated with any of their lengths. When a cracks reaches a morphology which has been defined as initiated crack it adds to the count of crack density ρ, being the number of cracks over the length of observation, which in this case is the observed length L of the side of the specimen.

$$\rho = \frac{n}{L}$$

The observation length influences the finding of results, as the first cracks may appear at very low crack densities. The observation length set for these experiments ranges around 40-50 mm. The criteria for choosing the equipment should be aligned with the expected damage size and inspection size. An example of characterization apparatus is reported from Ref. [14] in Figure 3, showing a side mounted microscope to measure cracks on a thermoplastic laminate. Crack along their length have been enclosed in rectangles for visualization purposes, it can be noted that not all of them spans trough the thickness of observed ply.

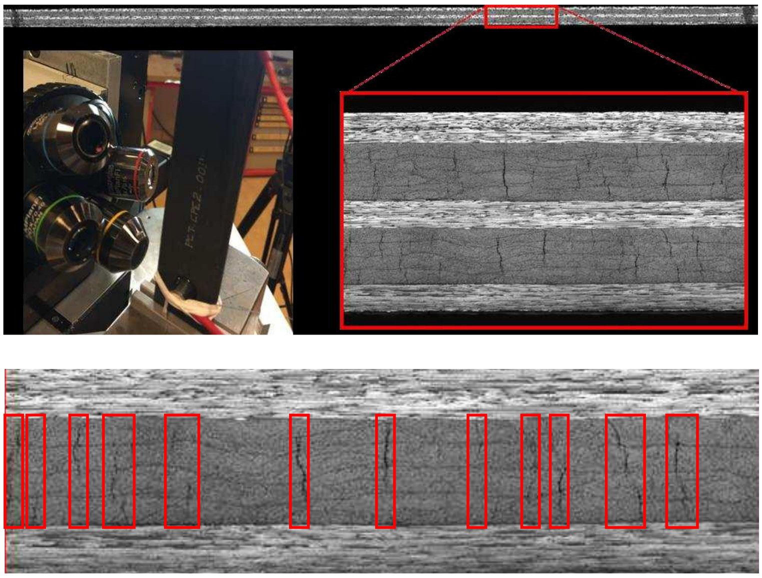

Figure 3 – Example adapted from Reference (Laurin, et al. 2023), thick laminate sample subject to static strain level. [02/904/0]s.

The number of cracks with a definite size (often this is the through thickness dimension) are then counted and related to the applied load and load cycles. What happens is that not all the cracks appear at the same time or in a linear way. The best representation for the crack formation trend has been proposed by Ref. [10], where a Weibull distribution of strengths to crack formation is attributed to the volume under examination. This is done for a static case, obtaining the regression shown in Figure 4.

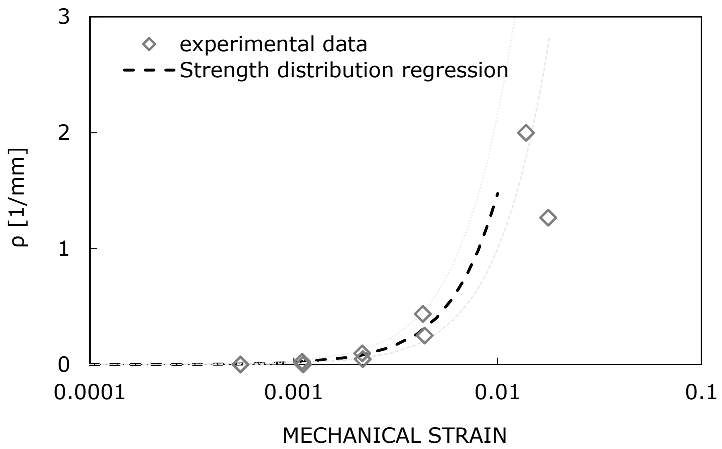

Figure 4 – Regression of crack density initiation on a specific ply of a laminate subject to tension in cryogenic environment.

Fatigue characterization should be performed in operational conditions to ensure the representativity of results. When the relationship between room temperature and cryogenic fatigue is clarified for the adopted material system, more economical tests could be sufficient.

3.3 Airworthiness evaluation methods

This section discusses methods to evaluate the tank's residual functionality when operational loading leads to the degradation phenomena discussed previously. Both a prognostic and a monitoring approach are discussed. Which approach is more suitable depends on the accuracy of the long-term material characterization and the accuracy of the load profiles.

Both methods ultimately evaluate the same performance indicator: the hydrogen permeability barrier requirement relative to alternative structural material classes. For polymer matrix composites, this requirement is intrinsically more demanding than for monolithic metals. The effective hydrogen diffusivity and solubility in polymers are several orders of magnitude higher than in dense metallic lattices, and, critically, the barrier performance does not scale favourably with increasing structural dimensions. Thickness increases provide only linear reductions in steady-state flux, while defect populations (microcracks, voids, fibre/matrix debond) statistically increase with part size, offsetting geometric gains. As a result, while permeation through composite laminates at room temperature can be low enough to be operationally negligible in small, pristine coupons, this behaviour is not directly transferrable to large, load-bearing cryogenic tanks.

Permeation behaviour is also strongly coupled to the operational strategy. Rapid chill-down, high fill rates, and frequent pressure cycling intensify thermomechanical gradients through the laminate thickness, promoting matrix microcracking and interfacial damage that create preferential diffusion pathways. Conversely, slow conditioning and limited cycling can maintain the material closer to its as-manufactured permeability state. Therefore, permeability cannot be treated as a purely intrinsic material property; it is a damage-state-dependent system parameter.

The emerging application of high-performance barrier coatings (e.g., thin inorganic or hybrid layers as discussed in [15]) introduces an additional transport-control mechanism but also a new failure mode hierarchy that is outside the present document's scope. Such coatings can reduce baseline hydrogen transmission by multiple orders of magnitude; however, as shown in earlier experimental work (e.g. Ref. [16]), their barrier efficiency is highly sensitive to cracking, debonding, and strain incompatibility with the underlying composite substrate. Even sub-visible crack networks can dominate overall permeability, effectively shifting the system from diffusion-controlled to defect-controlled transport.

A first-order justification for the permeation degradation approach adopted here is therefore to link barrier performance not only to pristine diffusivity data, but to mechanically driven damage evolution under representative cryogenic pressure cycling. This aligns with established durability methodologies in which transport properties are treated as state variables that evolve with crack density and connectivity rather than as fixed inputs [17].

Based on this framework, the working hypothesis in this section is that the intrinsic permeation of the uncoated, undamaged laminate is sufficiently low to prevent any operationally relevant loss of vacuum over the specified service intervals. Any vacuum degradation risk is thus assumed to arise primarily from damage-induced permeability increases rather than from the baseline material transport properties.

The foundations of hydrogen permeability research in composites were laid by early experiments showing helium and hydrogen transport in fibre-reinforced plastics. Measurements on glass/epoxy cryogenic composites demonstrated that gas permeability at room temperature is dominated by diffusion, but at cryogenic conditions leakage arises from cracking [18]. Similarly, thermal and mechanical cycling tests identified microcrack initiation as the limiting factor in barrier performance [19]. These works established the critical role of matrix integrity and fibre volume fraction in controlling baseline permeability values.

The early 2000s saw the first attempts to link crack mechanics with permeability in composites. Analytical and numerical studies introduced leakage models based on crack opening displacement, as seen in Refs. [20] and [21]; and on delaminated crack opening displacement [22], while biaxial cryogenic strain experiments highlighted the importance of microcrack networks in leakage formation [23]. These approaches were complemented by phenomenological descriptions of gas transport in polymers and composites [16], finite element approaches correlating crack density with permeability [24], and analytical formulations for leakage via delamination–microcrack overlap zones [25] and [26]. Together, these models established the conceptual framework that permeability in composites is governed not by pure diffusion, but by the creation and connection of microcracks and delaminations.

Experimental works have since provided clear evidence that once through-the-thickness cracks form, they dominate hydrogen transport. Matrix cracking under mechanical and cryogenic loads was shown to drastically increase leak rates [27] [28]. Tests on linerless tanks confirmed that microcracking is the principal barrier failure mode [29], [30]. More recently, detailed microstructural investigations under cryogenic cycling and pressurisation further validated this mechanism [31], [32]. For CF/PEEK laminates, manufacturing route and cryogenic cycling condition permeability [33], while thin-ply barrier layers provide enhanced resistance to cracking, such as seen in Refs. [34] and [35].

Alongside experiments, increasingly sophisticated modelling frameworks have emerged. Computational fluid dynamics based leakage simulations coupled with crack opening displacement and delamination parameters [36] were followed by multi-scale analytical methods incorporating crack opening mechanics [37]. Later, continuum damage mechanics was directly linked to permeability coefficients [38], while homogenization and effective diffusion tensor models extended permeability prediction to damaged laminates [39]. A particularly important advance was the use of extended finite element methods, first to model fatigue delamination and permeability under cryogenic cycling [40], and later to simulate random microcrack networks and leakage paths [41]. These models were validated against X-ray computed tomography observations of crack growth and experimental leak measurements, offering predictive tools that bridge damage mechanics and permeability.

Beyond cracking, permeability has also been shown to depend on microstructure, fibre–matrix interactions, and processing route. Investigations on thermoplastic laminates highlighted the strong influence of manufacturing method and fibre/matrix combinations on helium and hydrogen permeability [42]. Micro computed tomography based studies quantified how microcracks nucleate and connect under loading [43], while cryogenic strain–permeability coupling was confirmed experimentally [44] [45]. Together, these recent studies emphasize that laminate architecture, ply thickness, and structure integrity are fundamental in ensuring the composite barrier performance [46].

It should be noted that a comprehensive assessment of the influence of hydrogen on damage propagation, particularly under varying thermodynamic conditions such as sloshing, cooling, or warming, is required for the adopted laminate at higher technological maturity levels of the storage system. Within this context, a critical aspect of the evaluation concerns the selection of the design leak rate during fuelling of an empty tank. Under such conditions, the tank is expected to exhibit higher permeability compared to its cryogenic and steady state, due to elevated temperatures. However, as these behaviours are strongly dependent on operational choices, such as the specific fuelling procedure, their detailed investigation lies beyond the scope of the present document.

Please note that with this approach the change in permeation from the pristine state to a critical state are a fraction of the initial value, while when the last ply fails to a fully interconnected crack network the permeation values goes to infinity, signalling the change in hydrogen transport mode. For this reason, a criticality index should be maintained as well, defined as the maximum percentage of interconnected layer trough the tank thickness.

3.3.1 Simplified durability evaluation

The crack interconnection phenomenon occurs when one of the complete cracks in a layer intersects with a crack in an adjacent layer. This interaction can lead to the formation of a connected crack path between layers, ultimately resulting in the loss of containment for the whole structure. As the confidence in the analysis results increases, it becomes necessary to account for the probability of crack initiation within several single plies to evaluate the likelihood of such interconnection events.

A simplified analysis may focus on specific sections of the tank, named evaluation elements. When cracks extend through the thickness and the crack density in each ply exceeds 0.05 to 0.1 [1/mm] (about one crack every 10 to 20 mm), it can be assumed that the layers become interconnected, creating a continuous leak path. This assumption is supported by experimental evidence presented in Refs. [40] and [41], which shows through computed tomography (CT) investigations that already at this level, cracks are long enough to cross cracks in adjacent plies, in quasi-isotropic or cross-ply laminates with relatively thick plies. However, even in experimental tests where laminate thickness is smaller and comparable to the one used in the project, such as in Ref. [34], this value does not differ much. For lower crack densities, leak path formation becomes less probable as its evaluation would require a more in-depth characterization of the tunnelling propagation extent in cryogenic, fatigue conditions. Nevertheless, the surface manifestation of such cracks can still be leveraged for non-destructive evaluations.

With the aim to provide a conservative and still rapid tool to evaluate the permeation performance degradation following the formation of cracks in a tank structure, the following steps are taken. The max strain representing the characterization conditions can be calculated in elements with the size of 10-20 mm to comply with the initiation hypothesis introduced in the previous paragraph. This size determines the standard durability evaluation area, which is composed by several layers as represented in Figure 5. This simplified approach can be applied as long as stress does not vary significantly, or whenever local stress ratios does not hint at different failure mechanisms than transverse crack initiation, and usually considers only pressure, inertial and structural thermal loads, as thermal material loads are usually already considered within the characterization (A more accurate evaluation of thermal strains has to be considered when using characterisation data from one laminate type to predict the behaviour of another laminate type, as thermal strains are significantly higher in the cross-ply laminate compared to the quasi isotropic, given the change in coefficient of thermal expansion between layers). Another aspect is that the material is considered continuous in this analysis, while each interface, or discontinuous material such as ply changes, must be accounted as a seam when not properly analysed, and thus similar to a transverse crack.

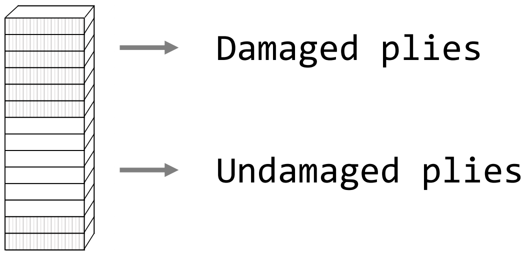

Figure 5 – Representation of a section of the laminate, with trough the thickness representation of the plies.

When a durability element is evaluated, the initiation of cracks is computed for each layer with the defined criteria, being static, fatigue, thermal or otherwise, as defined in the evaluation. In this section, the interest is in the result of the damage on the performance of the structure, so from now on the plies will be defined as damaged and undamaged. Undamaged plies will retain the permeability value of the pristine materials expressed in SI units as follows: $[\,\mathrm{mol} / (\mathrm{s} \cdot \mathrm{m} \cdot \mathrm{Pa})\,]$.

The residual molar permeation of the durability element can be calculated as the product between the permeability P of the material, the surface area A, which represents the area of the durability element through which the gas will permeate, thanks to the difference in pressure Δp between the two sides of the tank. The total thickness of the remaining intact plies $t_{undamaged}$ is in the dominator.

$$j = P \cdot \frac{A_{element} \cdot \Delta p}{t_{undamaged}} \qquad \left[\frac{\mathrm{mol}}{\mathrm{s}} \right]$$

Now we can add together the residual molar permeation of each different element composing the tank, which may have different degradation states, to the whole structure, obtaining the total flux of the tank. The leak rate terminology might be used now instead of permeation, as the only leak source is the permeation through the tank wall. (Usually the leak rate terminology includes permeation leaks plus leaks from interfaces, in this case no leaks from interfaces are currently considered).

$$j_{TOT} = \sum_{element} j_i \qquad \left[\frac{\mathrm{mol}}{\mathrm{s}} \right]$$

The tank flux can be converted from a molar rate to an occupied volume rate, to be able to understand the effect on the vacuum volume. By using the molar mass and the density of the permeating medium at the specific service condition the leak rate is:

$$J_{TOT} = j_{TOT} \cdot \frac{M_{H_2}}{\rho_{H_2}} \qquad \left[\frac{\mathrm{mbar} \cdot \mathrm{l}}{\mathrm{s}} \right]$$

This value can now be used to be compared with a threshold value for instantaneous evaluation such as:

$$J_{TOT} > J_{treshold} = 1e^{-9} \qquad \left[\frac{\text{mbar}\cdot\text{l}}{\text{s}}\right]$$

Given the tank structure leak rate also the "time to loss of vacuum" can be computed. This operation requires the knowledge of the vacuum volume V_{va} of the structure and the pressure limit to maintain the vacuum insulation, $P_{va,limit}$ with respect to the initial, or current, vacuum pressure p_{va}.

$$t_{va,loss} = V_{va} \cdot \frac{J_{TOT}}{p_{va,limit} - p_{va}} \qquad [\text{s}]$$

This last parameter is an important indicator of the residual life of the tank in service and a good aid during the design phase. Prognostic evaluations of the distributed fatigue formation of ply cracks can be translated to a reduced time to loss of vacuum, which will ultimately reach zero in critical conditions.

3.3.2 Monitoring of tank structural health

The possibility to detect and count cracks on specific points on the surface of the tank, thus relative to the external layer of the local laminate of a certain area, has been demonstrated within the project using Fibre Bragg Grating (FBG) optical sensor. This opens up to the possibility of monitoring the laminate damage, but the sensitivity of this method must be understood first. The following phenomena are discussed within this scope.

The sensor length influences the number of cracks that can be counted and thus the minimum crack density value, and an algorithm is required to convert the fibre optic spectra to crack count information.

It is accepted [47] that the external ply of a laminate is subject to earlier cracking with respect to the constrained plies subjected to the same strain level. This effect can be attributed to two main factors, one being the surface imperfection effect, while the other is the ply thickness effect. The first increases the number of nucleating sites, while the second facilitates the propagation of these into a full through the thickness crack. This phenomenon is favourable for the measurement of damage within the context of a cryogenic hydrogen tank, as measuring cracks on the outer layer does not mean that the inner plies are damaged.

The conformal shape makes the laminate stress vary significantly even among layers with the same orientation, leading to two aspects: a manageable damage allowance in some areas while distributed different stress behaviour are expected differently from a uniform, axisymmetric pressure cylinder.

The number of cracks measured by the sensor indicate the extent of damage. This information can be used in correlation to other laminate information to infer a local expected damage status.

4 References (Part I)

[1] A. K. Boddorff, "Choosing the Right Stuff: Material Selection for Liquid Hydrogen Aircraft Cryotanks," NASA STI Program Report Series, p. TM–20250007133, 2025.

[2] P. P. Parlevliet, H. E. Bersee and A. Beukers, "Residual stresses in thermoplastic composites – a study of the literature. Part III: Effects of thermal residual stresses," Composites Part A: Applied Science and Manufacturing, vol. 38, no. 6, pp. 1581-1596, 2007.

[3] G. Letchworth, "X-33 Reusable Launch Vehicle Demonstrator, Spaceport and Range," 2011.

[4] E. H. Glaessgen, J. R. Reeder, D. W. Sleight, J. T. Wang, I. S. Raju and C. E. Harris, "Debonding Failure of Sandwich-Composite Cryogenic Fuel Tank with Internal Core Pressure," Journal of Spacecraft and Rockets, vol. 42, no. 4, pp. 613-627, 2005.

[5] A. Hodge, "Evaluation of Microcracking in Two Carbon-Fiber/Epoxy-Matrix Composite Cryogenic Tanks," NASA/TM, vol. 211194, 2001.

[6] S. Choi and B. V. Sankar, "Micromechanical Analysis of Composite Laminates at Cryogenic Temperatures," Journal of Composite Materials, vol. 40, no. 12, pp. 1077-1091, 6 2006.

[7] A. Parvizi, K. Garret and B. J.E., "Constrained cracking in glass fibre-reinforced epoxy cross-ply laminates," JOURNAL OF MATERIALS SCIENCE, vol. 13, pp. 195-201, 1978.

[8] I. G. García, V. Mantič and A. Blázquez, "The effect of residual thermal stresses on transverse cracking in cross-ply laminates: an application of the coupled criterion of the finite fracture mechanics," International Journal of Fracture, vol. 211, no. 1–2, p. 61–74, 3 2018.

[9] M. Quaresimin, P. Carraro and L. Maragoni, "Early stage damage in off-axis plies under fatigue loading," Composites Science and Technology, vol. 128, pp. 147-154, 5 2016.

[10] P. Carraro, L. Maragoni and M. Quaresimin, "Prediction of the crack density evolution in multidirectional laminates under fatigue loadings," Composites Science and Technology, vol. 145, pp. 24-39, 6 2017.

[11] P. A. Carraro, M. Simonetto and M. Quaresimin, "Fatigue damage evolution in glass/epoxy cross-ply laminates under spectrum loadings," Composites Part A: Applied Science and Manufacturing, vol. 173, p. 107680, 10 2023.

[12] C. Lüders and M. Sinapius, "Fatigue of fibre-reinforced plastics due to cryogenic thermal cycling," Journal of Composite Materials, vol. 53, no. 20, p. 2849–2861, 1 2019.

[13] M. Quaresimin, P. A. Carraro, L. Maragoni and M. Simonetto, "Experimental analysis and modelling of fatigue crack initiation in glass/epoxy laminates with stress concentrations," International Journal of Fatigue, vol. 201, p. 109135, 2025.

[14] F. Laurin, A. Mavel, J.-M. Garcia and M. Herman, "Experimental and numerical study on the transverse cracking in a composite material with a thermoplastic matrix," in Composites Meet Sustainability – Proceedings of the 20th European Conference on Composite Materials, ECCM20., Lausanne, Switzerland, 2023.

[15] E. Akbari-Kharaji, M. Shafaie, E. Sackett, J. Wood, M. B. Djukic and S. Alexander, "Hydrogen barrier coatings: Application and assessment," International Journal of Hydrogen Energy, vol. 180, no. 0360-3199, p. 151666, 2025.

[16] D. Schultheiß, Permeation Barrier for Lightweight Liquid Hydrogen Tanks, OPUS Augsburg: Dissertation zur Erlangung des Doktorgrades der Mathematisch-Naturwissenschaftlichen Fakultat der Universitat Augsburg, 2007.

[17] Y. Li, J. Meng, J. Luo, P. Wang, J. Ma, Z. Zhao and H. Lei, "Cryogenic mechanics and damage behaviors of carbon fiber reinforced polymer composites," Composites Part A: Applied Science and Manufacturing, vol. 169, p. 107484, 6 2023.

[18] S. Disdier, J. Rey, P. Pailler and A. . Bunsell, "Helium permeation in composite materials for cryogenic application," Cryogenics, vol. 38, no. 1, pp. 135-142, 1998.

[19] J. Humpenoder, "Gas permeation of fibre reinforced plastics," Cryogenics, vol. 38, no. 1, pp. 143-147, 1998.

[20] H. Kumazawa, T. Aoki and I. Susuki, "Analysis and Experiment of Gas Leakage Through Composite Laminates for Propellant Tanks," AIAA Journal, vol. 41, no. 10, pp. 2037-2044, 10 2003.

[21] P. Peddiraju , P. Popov, J. Whitcomb and D. C. Lagoudas, "CHARACTERIZATION OF EFFECTIVE PERMEABILITY IN CRYOGENIC COMPOSITE LAMINATES," in ASME INTERNATIONAL MECHANICAL ENGINEERING CONGRESS & EXPOSITION , WASHINGTON, D.C., 2003.

[22] S. Roy and M. Benjamin, "Modeling of permeation and damage in graphite/epoxy laminates for cryogenic fuel storage," Composites Science and Technology, vol. 64, no. 13–14, p. 2051–2065, 10 2004.

[23] E. Stokes, "Hydrogen Permeability of Polymer Based Composites Under Bi-axial Strain and Cryogenic Temperatures," in 45th AIAA/ASME/ASCE/AHS/ASC Structures, Structural Dynamics Materials Conference, 2004.

[24] J. Xu and B. V. Sankar, "Parametric Investigation of Gas Permeability in Cross-Ply Laminates Using Finite Elements," AIAA Journal, vol. 45, no. 4, pp. 934-941, 2007.

[25] T. Yokozeki, T. Aoki and T. Ishikawa, "The effect of matrix cracks on gas permeability through CFRP laminates," Advanced Composite Materials, vol. 13, no. 3–4, p. 227–236, 1 2004.

[26] R. Grenoble and T. Gates, "Hydrogen Permeability of Polymer Matrix Composites at Cryogenic Temperatures," in 46th AIAA/ASME/ASCE/AHS/ASC Structures, Structural Dynamics and Materials Conference, 2005.

[27] H. Kumazawa, H. Hayashi, I. Susuki and T. Utsunomiya, "Damage and permeability evolution in CFRP cross-ply laminates," Composite Structures, vol. 76, no. 1–2, p. 73–81, 10 2006.

[28] T. Yokozeki, T. Ogasawara, T. Aoki and T. Ishikawa, "Experimental evaluation of gas permeability through damaged composite laminates for cryogenic tank," Composites Science and Technology, vol. 69, no. 9, pp. 1334-1340, 7 2009.

[29] K. Mallick, M. Tupper, B. Arritt and C. Paul, "Thermo-Micromechanics of Microcracking in a Cryogenic Pressure Vessel," in 44th AIAA/ASME/ASCE/AHS/ASC Structures, Structural Dynamics, and Materials Conference, 2003.

[30] J. Ju, B. D. Pickle, R. J. Morgan and J. Reddy, "An Initial and Progressive Failure Analysis for Cryogenic Composite Fuel Tank Design," Journal of Composite Materials, vol. 41, no. 21, pp. 2545-2568, 11 2007.

[31] C. Rauh, T. Reimer and J. Wilken, "LEAKAGE INVESTIGATION OF EPOXY-BASED COMPOSITE LAMINATES FOR REUSABLE CRYOGENIC PROPELLANT TANKS," in 2nd International Conference on Flight Vehicles, Aerothermodynamics and Re-entry Missions & Engineering (FAR), Heilbronn, Germany, 2022.

[32] S. Liu, L. Zhan, B. Ma, C. Guan and X. Yang, "Simulation and Experimental Study on the Internal Leak Behavior in Carbon Fiber Reinforced Composite Components," Polymers, vol. 15, no. 13, p. 2758, 6 2023.

[33] M. Flanagan, D. Grogan, J. Goggins, S. Appel, K. Doyle, S. Leen and C. Ó Brádaigh, "Permeability of carbon fibre PEEK composites for cryogenic storage tanks of future space launchers," Composites Part A: Applied Science and Manufacturing, vol. 101, p. 173–184, 10 2017.

[34] H. Hamori, H. Kumazawa, R. Higuchi and T. Yokozeki, "Gas permeability of CFRP cross-ply laminates with thin-ply barrier layers under cryogenic and biaxial loading conditions," Composite Structures, vol. 245, p. 112326, 8 2020.

[35] I. Katsivalis, V. Signorini, F. Ohlsson, C. Langhammer, M. Minelli and L. E. Asp, "Hydrogen permeability of thin-ply composites after mechanical loading," Composites Part A: Applied Science and Manufacturing, vol. 176, p. 107867, 1 2024.

[36] H. Kumazawa and J. Whitcomb, "Numerical Modeling of Gas Leakage Through Damaged Composite Laminates," Journal of Composite Materials, vol. 42, no. 16, pp. 1619-1638, 8 2008.

[37] C. Bois, J.-C. Malenfant, J.-C. Wahl and M. Danis, "A multiscale damage and crack opening model for the prediction of flow path in laminated composite," Composites Science and Technology, vol. 97, pp. 81-89, 2014.

[38] R. Bogenfeld, C. Lüders, M. Ebermann and V. Ravi, "A direct correlation between damage parameters and effective permeation coefficients in composite laminates," Composites Part A, vol. 185, p. 108307, 2024.

[39] M. Ebermann, R. Bogenfeld, J. Kreikemeier and R. Glüge, "Analytical and numerical approach to determine effective diffusion coefficients for composite pressure vessels," Composite Structures, vol. 291, p. 115616, 2022.

[40] D. Grogan, S. Leen, C. Semprimoschnig and C. Ó Brádaigh, "Damage characterisation of cryogenically cycled carbon fibre/PEEK laminates," Composites Part A: Applied Science and Manufacturing, vol. 66, p. 237–250, 11 2014.

[41] D. Grogan, C. Ó Brádaigh, J. McGarry and S. Leen, "Damage and permeability in tape-laid thermoplastic composite cryogenic tanks," Composites Part A: Applied Science and Manufacturing, vol. 78, p. 390–402, 11 2015.

[42] J. Conde-Wolter, M. G. Ruf, A. Liebsch, T. Lebelt, I. Koch, K. Drechsler and M. Gude, "Hydrogen permeability of thermoplastic composites and liner systems for future mobility applications," Composites Part A: Applied Science and Manufacturing, vol. 167, p. 107446, 4 2023.

[43] J. Meng, H. Zheng, Y. Wei, D. Liu, H. Shi, P. Wang, H. Lei and D. Fang, "Leakage performance of CFRP laminate under cryogenic temperature: Experimental and simulation study," Composites Science and Technology, vol. 226, p. 109550, 7 2022.

[44] S. Saha, R. W. Sullivan and M. L. Baker, "Gas permeability of three-dimensional stitched carbon/epoxy composites for cryogenic applications," Composites Part B: Engineering, vol. 216, p. 108847, 7 2021.

[45] M. Yuan, H. Zhao, Y. Peng, L. Tian, Y. Yao and J. Chen, "Numerical Method for Predicting Permeability of Laminated Composites at Cryogenic Temperature," AIAA Journal, vol. 59, no. 7, p. 2784–2792, 7 2021.

[46] S. Saha and R. W. Sullivan, "A review on gas permeability of polymer matrix composites for cryogenic applications," Journal of Composite Materials, vol. 58, no. 6, pp. 827-847, 1 2024.

[47] J. A. Nairn and S. Hu, "The Formation and Effect of Outer-Ply Microcracks in Cross-Ply Laminates: A Variational Approach," Engineering Fracture Mechanics, vol. 41, pp. 203-221, 1992.

Part II: Life Cycle Analysis

5 Introduction - LCA

Despite its continuous growth over the years, aviation is frequently criticized for its high greenhouse gas emissions and ecological footprint [1,2]. In response, several major companies and research initiatives are aiming to drastically reduce the sector's environmental impact. One promising solution is the use of hydrogen as an alternative aviation fuel [3–8], offering the potential for net-zero emissions at use in the future [3,9]. Additionally, hydrogen exhibits a high gravimetric energy density [10,11], i.e., it stores more energy per kilogram of material compared to traditional fuels. It is especially a critical advantage for the aviation sector, which is highly sensitive to weight. However, hydrogen also suffers from an extremely low volumetric energy density [10,11] at ambient temperature and pressure, posing significant challenges for onboard storage.

Thus, a key challenge in enabling hydrogen-powered aviation lies in the efficient onboard storage of hydrogen. To address this, several storage technologies have been developed [10–14]. Most widely used approach is storage as compressed gas in a pressure vessel [10,15]. Other methods include storage in liquid form at cryogenic temperatures [16,17], a hybrid approach such as cryo-compressed storage [18], and solid-state storage in the forms of metal or chemical hydrides [19]. To achieve the high volumetric energy density required for aviation or aerospace applications, hydrogen is most effectively stored in its liquid form at cryogenic temperatures. With its significantly higher density than compressed hydrogen, liquid hydrogen enables storage in smaller tanks and makes it a favourable option [12,16].

Traditionally, to store liquid hydrogen at cryogenic temperatures, tanks have been manufactured from metals, predominantly various grades of stainless steel. However, steels are susceptible to hydrogen embrittlement, which has driven research into alternative materials. Aluminium-based and titanium-based alloys have been explored as substitutes, as they mitigate embrittlement. However, aluminium presents challenges related to welding and joining techniques, while titanium is expensive and exhibits degradation in certain mechanical properties at cryogenic temperatures [20]. Moreover, though metal-based tanks are suitable for ground-based applications, they are relatively heavy for aviation and aerospace uses, where weight is a critical design constraint. In this context, fibre-reinforced polymer (FRP) composites have emerged as a promising alternative. These materials offer significant weight reduction and are increasingly regarded as one of the most viable solutions for future liquid hydrogen storage systems [20].

However, traditional storage solutions are typically designed as cylindrical or spherical tanks, which excel in providing uniform stress distribution, but do not utilize the available aircraft volume efficiently. The Composite Conformal Liquid H_2 Tank (COCOLIH2T) project [21] seeks to address this issue by developing a conformal tank that fits within the contours of the aircraft fuselage. Such a design aims to improve space utilization in aircrafts and free up internal space for other aircraft systems, including passenger seating. This novel tank is designed using thermoplastic carbon fibre reinforced polymers (CFRP) and manufactured through automated fibre placement (AFP). Unlike conventional filament winding (FW), which imposes limitations on fibre orientation and layup design, AFP enables precise control of fibre angles and allows region-specific layup tailoring, offering greater flexibility to optimize structural performance. In addition, the use of thermoplastic composite materials rather than conventional thermoset systems offers the advantage of recyclability, thereby improving the environmental sustainability of the tank over its entire life cycle.

As environmental sustainability is a primary motivation for the adoption of hydrogen in aviation, it is essential to critically evaluate whether emerging hydrogen storage technologies genuinely advance sustainability objectives or accidentally introduce new environmental burdens. This includes assessing the life cycle impact of the innovative design proposed by the COCOLIH2T project in comparison to conventional cylindrical tanks made with thermoset resin.

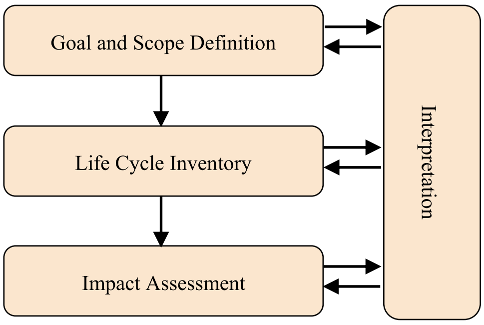

Figure 6 Stages of Life Cycle Assessment

In this regard, life cycle assessment (LCA) is a valuable tool for systematically evaluating the environmental impact of a product throughout its lifespan. The structured approach for conducting LCA involves four distinct stages, as shown in Figure 6. Goal and scope definition, the first stage in LCA, involves two primary tasks: defining the functional unit (the quantified reference for comparing environmental impacts of products) and establishing the system boundary (the extent of the product's life cycle stages and processes considered for analysis). The next stage is life cycle inventory, which involves the collection of the data needed to perform the analysis. It includes, but is not limited to, material quantification, energy consumption during manufacturing, transportation and service life, form of the energy used, environmental discharges and disposal pathways of the material. Once the inventory is created, impact assessment is performed to gain the insights about the environmental impacts associated with the system in consideration. In this stage, the data obtained during the inventory stage for the several environmental impacts is analysed and categorised into specific impact categories. The interpretation stage in LCA is connected to all other three stages. It deals with systematic evaluation of the LCA results to derive meaningful conclusions and recommendations.

Most studies evaluating the environmental impact (in some cases, the energy requirements) of hydrogen storage options primarily focus on pressurised storage of hydrogen in metallic or composite pressure vessels [22–31]. A few investigations also consider solid-state storage methods, such as metal hydrides [24,25,30]. In particular, studies dedicated to the LCA of cryogenic liquid hydrogen storage vessels are minimal in the literature [22,25,30,31]. Among the limited available research, most focus on metallic vessels [25,30,31] or metal-lined composite vessels [22]. Moreover, these studies often centre around broader applications, such as fuel cell vehicles or hydrogen production, where hydrogen storage is treated as a secondary component in the LCA study. As a result, detailed LCA specifically targeting the environmental impact of the storage tanks themselves are relatively uncommon.

The objective of this study is to address that gap by performing a comparative LCA of two liquid hydrogen storage tanks: a traditional cylindrical tank (referred to as the baseline tank) and the novel conformal COCOLIH2T tank. The two tanks differ in three critical aspects: geometry, manufacturing method, and resin type. The baseline tank is cylindrical, manufactured via FW, and made of carbon fibre reinforced epoxy (CF/Epoxy), a thermoset resin. In contrast, as mentioned earlier, the COCOLIH2T tank is conformal in shape, produced using AFP, and constructed from carbon fibre reinforced poly-aryl-ether-ketone (CF/PAEK), a thermoplastic resin.

The environmental impacts of both designs are evaluated across eighteen distinct impact categories, offering a comprehensive assessment that goes beyond the commonly evaluated global warming potential. Impacts are first quantified for the production phase using a cradle-to-gate approach, which covers the life cycle from raw material extraction to the factory gate, corresponding to the completed manufacture of the tanks. Subsequently, a cradle-to-grave analysis is conducted to capture the full life cycle, incorporating both the production phase and end-of-life (EoL) treatment of materials. Two EoL scenarios are examined: (i) disposal via landfill and (ii) a circular strategy emphasizing recycling and, where applicable, energy recovery through incineration.

Insights has been drawn from this study about the trade-offs between thermoplastic and thermoset composites, baseline and COCOLIH2T tank, and informed material and design choices for sustainable hydrogen storage in aviation.

6 Methodology

6.1 Goal and scope definition

The goal of this study is to evaluate the environmental impact of a newly proposed conformal liquid hydrogen storage tank (COCOLIH2T tank) and to compare its performance with that of a conventional cylindrical storage tank (baseline tank). A representative geometry for both the tank designs is showcased in Figure 7 (The images are provided solely for visual reference and do not represent accurate dimensions or final design details). Both designs are intended to store the same volume of hydrogen at cryogenic temperature and are manufactured using CFRP materials. Each tank consists of a double-vessel configuration, comprising an inner vessel and an outer vessel separated by a vacuum layer to minimise heat transfer and hydrogen boil-off.

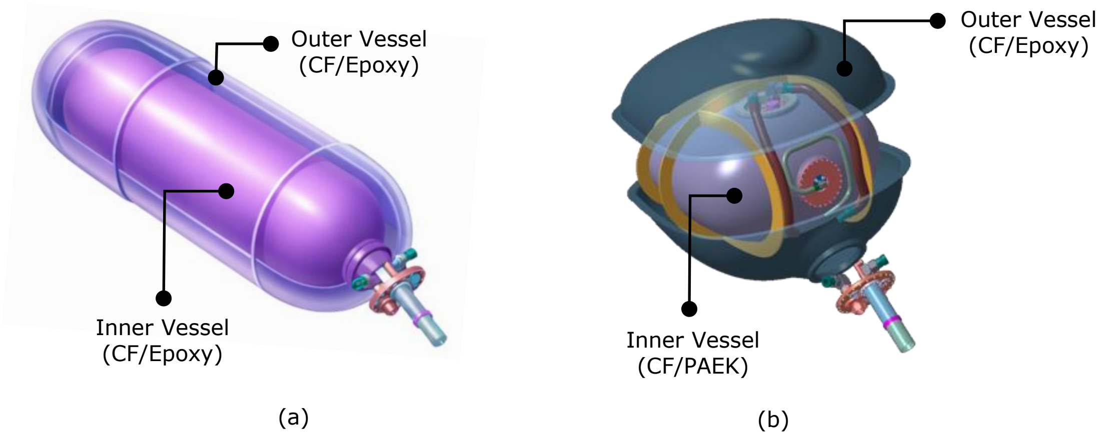

Figure 7. Representative geometry of (a) baseline tank (image created using generative AI) and (b) COCOLIH2T tank

The functional unit for the LCA of the production phase is defined as the production of one unit of storage tank. The scope of this study follows a cradle-to-gate approach, encompassing all processes from raw material extraction to the completion of manufacturing at the factory gate. Detailed descriptions of the production processes for both tank configurations are provided in the subsequent subsections.

For the cradle-to-grave LCA, functional unit is defined as the production and disposal of one unit of storage tank. The system boundary here encompasses raw material extraction, component manufacturing, and EoL treatment. The use phase is excluded from the study, as both tanks are assumed to provide equivalent functional performance during operation. For the end-of-life strategies, the study explicitly considers two variations in order to assess influence of disposal pathways on the overall environmental impact. The first scenario, termed as *Scenario-1*, represents a case in which all materials are assumed to be landfilled without any material or energy recovery. The second scenario, termed as *Scenario-2*, reflects current commercially available recycling and energy recovery pathways. By considering these two EoL scenarios, the study provides a range for the potential environmental impacts associated with each tank design. Details about EoL strategy used for each specific component of the tank are provided in the subsequent subsections.

6.1.1 Designing, production and disposal of COCOLIH2T Tank

The conformal COCOLIH2T tank has been specifically developed and designed to fit within the fuselage of an ATR-72 aircraft, with a goal of storing 57 kg of hydrogen in liquid state. The shape and layup the of inner vessel are optimised to maximise the utilization of the available space within the aircraft while minimizing overall weight. In addition to fulfil mechanical and thermal performance requirements, constraints related to the maximum allowable boil-off and hydrogen leakage are also considered during the design process. A representative illustration of the COCOLIH2T tank geometry is provided in Figure 7 (b).

The inner vessel of the COCOLIH2T tank is manufactured from CF/PAEK, using AFP. AFP provides better control over layup angle and thus, it is possible to locally reinforce the sections of the tank, based on the stress distribution. The mandrel required for this process is constructed from steel. The outer vessel is manufactured using thermoset composite, CF/Epoxy, via hand-layup process over a mold made from the same composite material. This mold, also created using hand-layup process, is in turn produced using a medium-density fibreboard (MDF) super-mold, which serves as a form for the final composite mold. All components produced using CF/Epoxy goes through the curing process in an autoclave.

For the disposal, in Scenario-1, all materials, i.e., CF/PAEK, CF/Epoxy, steel, and MDF, go towards the landfill. Whereas, in Scenario-2:

- The Steel mandrel is assumed to be recycled and reused in new steel production via electric arc furnace processes.
- MDF is sent to incineration facilities for heat and electricity recovery.
- Thermoset CFRP waste is assumed to be incinerated for energy recovery, reflecting current limitations in large-scale recycling of thermoset composites.
- In contrast, thermoplastic CFRP components are assumed to be mechanically recycled by shredding and reprocessing into pellets, which can then be reused in manufacturing processes such as injection molding or compression molding as short-fibre-reinforced composites.

Figure 8 presents an overview of the COCOLIH2T tank manufacturing and disposal processes and highlights the scope of LCA study for both EoL scenarios. The boundaries of the production phase are also highlighted separately in the figure.

6.1.2 Designing, production and disposal of baseline Tank

The baseline tank is designed to match the internal volume of the COCOLIH2T tank (to store 57 kg of hydrogen), ensuring that the operational range of the aircraft remains unaffected. The radius of the tank is determined by the available space within the aircraft fuselage, which, given the fixed volume requirement, in turn dictates the tank's length. Based on this, the tank is designed with a diameter of 800 mm and the length of 2000 mm for the cylindrical portion.

Instead of developing a fully detailed design, a simplified design procedure is employed for the baseline tank with an objective to determine a suitable constant wall thickness that meets the functional requirements and allows for accurate estimation of material consumption. The major design criteria is that the tank must withstand an internal pressure of 8 bar, i.e., 0.8 MPa along with the stresses induced due to cryogenic cooling. It should be noted that any thermal gradients along the thickness of the wall are not considered during the design. Thermal stresses appear because of differential shrinkage (or expansion) in the different layers because of the layup angle and directional nature of the coefficient of thermal expansion. Furthermore, to prevent leakage due to microcracks or material permeability, thickness of the inner vessel is needed to be a minimum of 5 mm, which ensures sufficient hydrogen containment.

Finite element simulations were performed to evaluate the mechanical performance under these conditions. The analysis confirmed that a wall thickness of 5 mm is sufficient to meet the pressure and thermal load constraints. Consequently, this value was adopted for the final design. Since LCA calculations are based on the total quantity of the material used rather than the specific layup sequence of the laminates, the latter is not a matter of importance here. For the outer vessel, a separate structural design was not conducted. Instead, the same wall thickness of 4.8 mm, as that of the COCOLIH2T outer vessel, which was already designed to resist external pressure and prevent buckling, was used for the baseline configuration.

The manufacturing process of the baseline tank largely mirrors that of the COCOLIH2T tank, with two key distinctions. First, the inner vessel is fabricated using filament winding instead of AFP. Second, the baseline tank utilises thermoset composites for both the inner and outer vessels, eliminating the use of thermoplastics. As a result, autoclave curing is required for both inner and outer vessel.

For the disposal, similar to COCOLIH2T tank, in Scenario-1 assumes that all materials are sent to landfill. In contrast, Scenario-2 assumes that steel is recycled, while MDF and CF/Epoxy are incinerated for energy recovery.

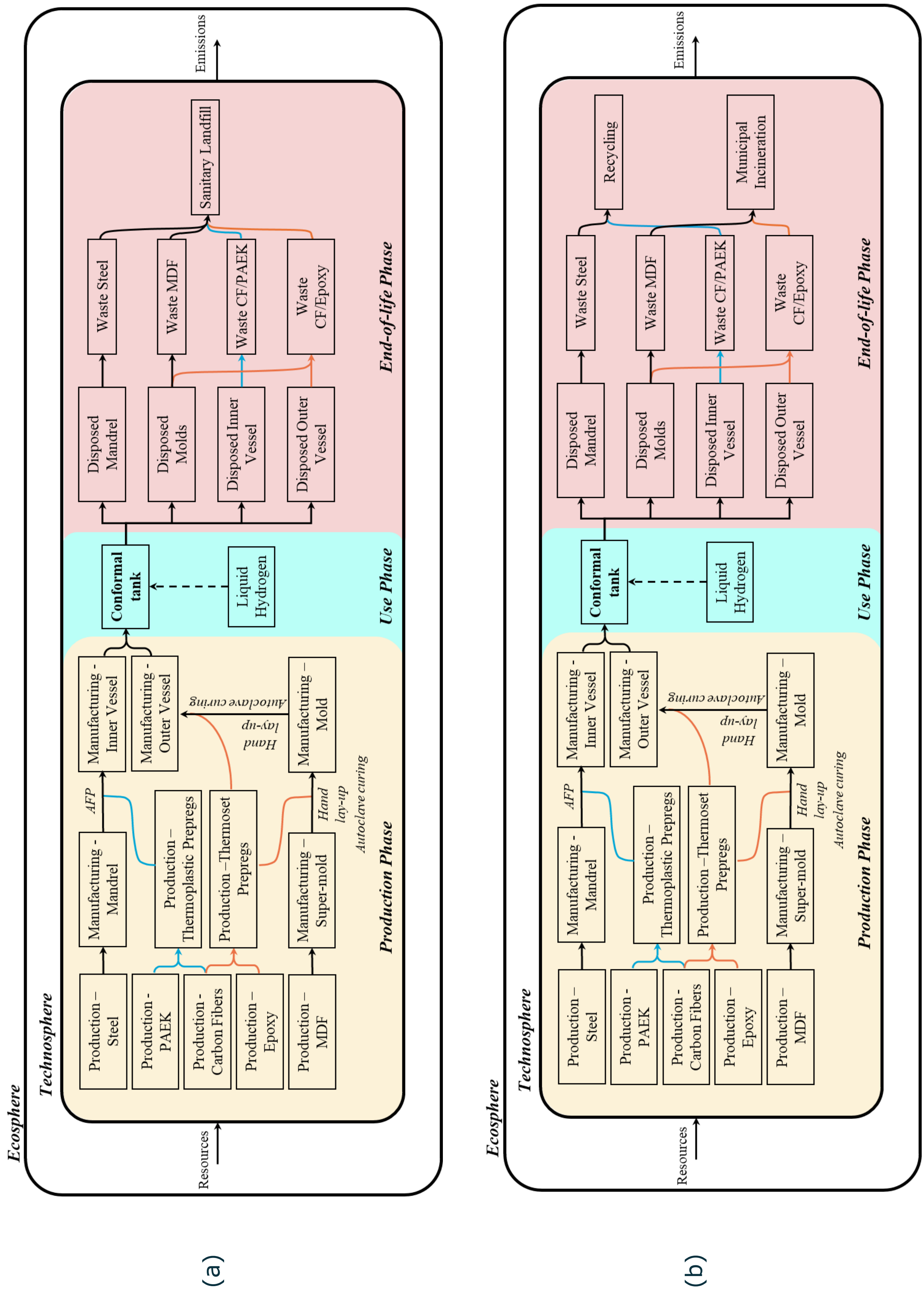

Figure 8. Schematic representation of the life cycle of the COCOLIH2T Tank, (a) EoL Scenario-1 and (b) EoL Scenario-2

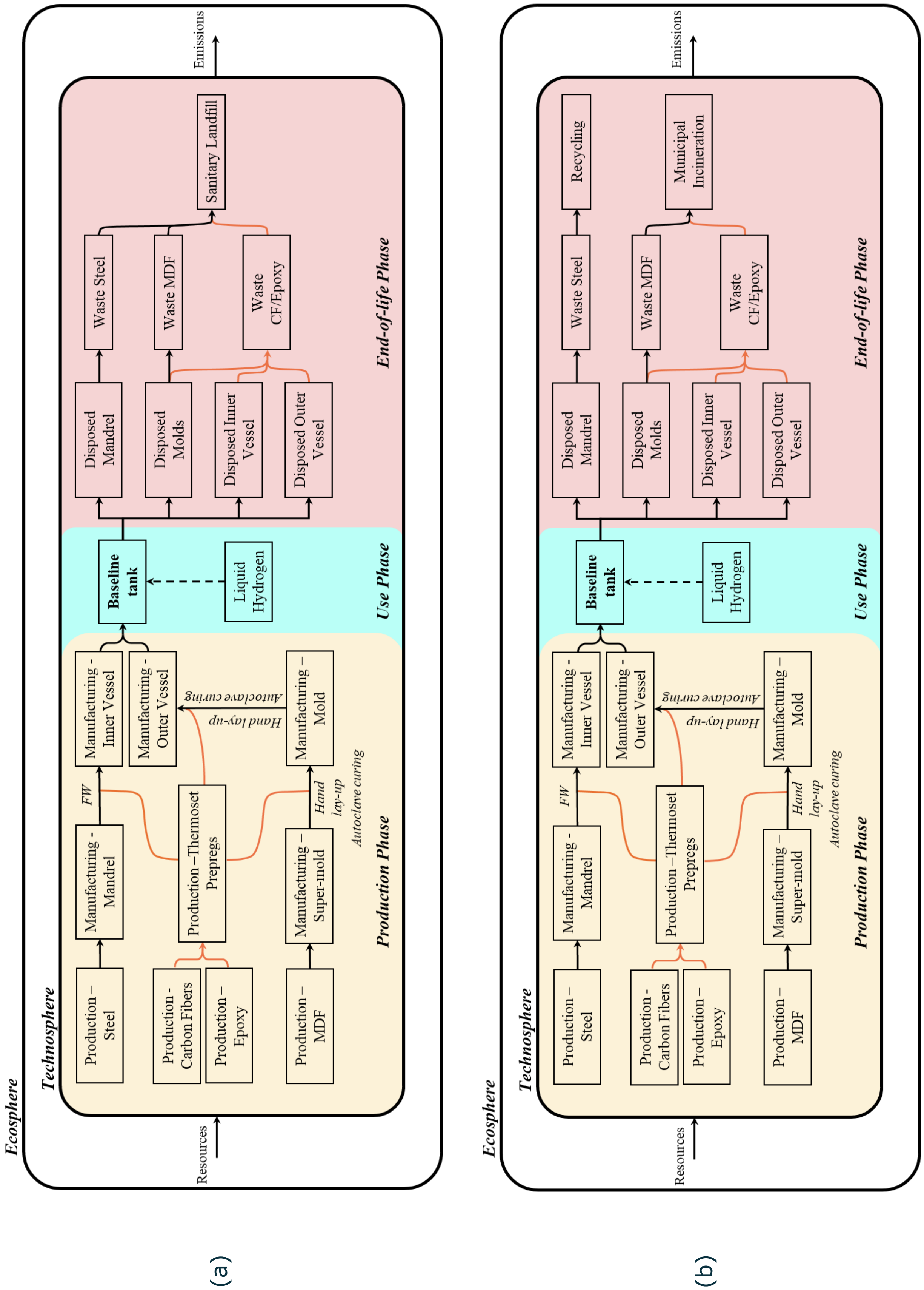

Figure 9. Schematic representation of the life cycle of the baseline Tank, (a) EoL Scenario-1 and (b) EoL Scenario-2

A schematic of the baseline tank manufacturing as well as disposal process is shown in Figure 9, which also captures the scope of LCA study for both EoL Scenarios. The scope of the LCA of production phase is also highlighted separately in the figure with different boundaries.

Though, it should be noted that use phase showcasing consumption of hydrogen is included in the figures (Figure 8 and Figure 9, both) only for completeness and is not considered in the analysis, thus, is shown with a dashed line. Additional details regarding life cycle inventory data, modelling assumptions, and end-of-life pathways are provided in the further sections of this report as well as in the provided supplementary material.

6.2 Background database

To perform a robust and comprehensive life cycle assessment, it is essential to gather a wide range of background inventory data representing upstream and downstream processes that are not directly modelled within the foreground system. This background data includes information on raw material extraction, energy production, transportation, manufacturing processes and emissions. It plays a critical role in capturing the indirect environmental impacts associated with the product under study. In this study, the Ecoinvent database (version 3.8) [32,33] is used as the source for the background data.

Among the system models available within the Ecoinvent database, which defines the rules for allocating environmental burden across various actors, the 'cut-off by classification' model is employed within this study. This model is based on 'polluter pays' principle, and hence, waste is considered the responsibility of its producers. Under this approach,

- Recyclable materials are cut-off from their upstream environmental burdens at the point of their collection or treatment. As a result, they are treated as burden-free resources for recycling facilities and for further use, with no environmental credit granted to the original producer. Consequently, the environmental impacts associated with the production of virgin materials are fully allocated to the primary manufacturer [34].
- In case of waste materials with no value or potential for recycling, which must be discarded via landfill or incineration, or might require pre-treatment before discarding, the responsibility similarly lies with the waste producer. Thus, the producer bears complete responsibility for any waste generated and its subsequent treatment. Additionally, any valuable by-products generated during waste treatment, such as heat or electricity from incineration, are also cut-off from the original system and made available to use without environmental burden for downstream use, again providing no credit to the primary producer.

However, to properly reflect the end-of-life (EoL) strategies considered in this study, credits associated with material recycling and energy recovery from incineration must be included. Therefore, a system expansion approach was applied in the analysis. Through system expansion, environmental credits are assigned for the avoided production of virgin materials and conventional energy by explicitly modelling these substitutions. This approach allows the benefits of recycling and energy recovery to be reflected in the results, effectively overriding the default cut-off by classification treatment, while maintaining consistency with the overall modelling framework.

6.3 Impact assessment method

Several impact assessment methods are available for conducting LCA, including ReCiPe, TRACI, ILCD, and CML [35]. These methods have been developed in different regions of the world, reflecting local environmental priorities, electricity grids, and other regional conditions. As a result, they differ in how they categorise environmental impact categories. In this study, the ReCiPe 2016 v1.1 method is used, as it was developed in the Netherlands for the application in the European context. Since the manufacturing is being performed in Europe, primarily in Italy, ReCiPe is considered the most suitable method.

Impact assessment methods may follow either a midpoint or an endpoint modelling approach [36,37]. The two differ in where they evaluate environmental impacts along the cause-effect chain (environmental mechanism). The midpoint method evaluates impact at earlier stages, which makes them more scientifically robust and easier to measure. Midpoint indicators focus on specific environmental issues, such as climate change or acidification, but they are less directly linked to actual environmental damage outcomes. In contrast, the endpoint method assesses impact closer to the final environmental outcomes, offering more intuitive and policy-relevant results. However, it generally involves greater uncertainty and reduced verifiability [36,37]. With version 1.1, the ReCiPe method provides eighteen impact categories for midpoint indicators, with marine eutrophication added to the list compared to the previous version with seventeen categories [38–40]. Whereas, its endpoint indicators aggregate the impacts into three broader categories, human health, biodiversity, and resource scarcity [38–40]. However, as each aggregation step introduces more uncertainty, midpoint indicators are preferred for the analysis in this study.

Another important aspect of the ReCiPe method is the choice of perspective. There are three available perspectives, Individualist (I), Hierarchist (H), and Egalitarian (E) [39,40]. These perspectives differ primarily in the time horizons they consider. The Individualist perspective focuses on short-term impacts (approximately 20 years) and tends to be more optimistic, assuming that future technological advancements will mitigate long-term consequences. The Hierarchist perspective, which is commonly used in LCA studies, reflects a balanced, science-based approach with a time horizon of about 100 years. It is grounded in current scientific consensus and established policy targets. In contrast, the Egalitarian perspective adopts a long-term or even permanent outlook, often spanning thousands of years, and takes a precautionary stance aimed at protecting the environment for future generations. In line with most LCA studies, this study adopts the Hierarchist (H) perspective. Therefore, the environmental impact assessment is conducted using *'ReCiPe 2016 v1.1 Midpoint (H)'* method. For normalization, this study uses factors provided by the ReCiPe method, based on the 2010 per capita world averages, following the Hierarchist perspective for midpoint categories. OpenLCA, an open access software tool available to conduct LCA, is used to develop the model and perform the calculations.

7 Life cycle inventory

The collection of data for inventory development is a critical step in conducting a life cycle assessment. The reliability of the assessment heavily depends on the accuracy of the input data. Without accurate and representative data, the results of the LCA may hold little to no value. Although numerous databases are available, they cannot be exhaustive and may not always provide the specific information required. Additionally, it is also not always feasible to obtain first-hand information related to the material and energy consumption during the production and life cycle of a certain product. In such cases, it becomes necessary to rely on well-informed estimations to approximate real-world conditions and derive representative values. These estimates were carefully selected to minimise their influence on the inferred outcomes of the analysis.

7.1 Assumptions

Given the comparative nature of this study, the modelling effort focuses on components and processes that significantly differentiate the two tank designs. Elements, such as insulation layers or spacers, that are common to both designs and are expected to have a marginal contribution to the overall environmental impacts were excluded to avoid unnecessary complexity. The major assumptions adopted in the LCI modelling are summarised below.

7.1.1 Assumptions related to level of detail

The following assumptions reflect deliberate modelling choices regarding the level of detail included in the LCI. These exclusions are justified either because their contribution to the total environmental impact is expected to be minor or because they are identical for both tank designs and therefore do not affect the comparative conclusions.

- Supporting components of the tank system, such as spacers, thermal insulation, valves, and ancillary fittings, are excluded. The analysis focuses exclusively on the primary structural components, the inner and outer vessels.
- Scrap and waste materials generated during manufacturing processes are not considered.
- Autoclave consumables, including vacuum bags, peel plies, hoses, and release films, are excluded from the inventory.

7.1.2 Assumptions due to data limitations

Certain assumptions were required due to the lack of detailed information for specific processes or materials. Once again, these assumptions are considered to have a limited influence on the final results or will provide similar contributions to both tank designs, thus, do not alter the overall trends or conclusions.

- The specific manufacturing techniques and associated energy consumption for the production of the mandrel and super-mold are not known; therefore, energy inputs related to their manufacturing are not included in the analysis.
- Transportation-related emissions are indirectly represented using market activity datasets available in the Ecoinvent database, without any explicit consideration. It is assumed that, under commercial production conditions, manufacturing facilities would be located in proximity to one another, resulting in a relatively small contribution of transportation to the overall environmental impact.
- Background databases do not include inventory data for PAEK production. Since PEEK belongs to the same polymer family and exhibits similar material properties, it is used as a proxy material in the analysis.

7.1.3 Others assumptions

- The use-phase inventory does not account for hydrogen consumption and hence, hydrogen production is also excluded from the system boundaries.
- For mandrel and molds,
    - **Production phase LCA**: As the production is considered to be carried out at laboratory scale and involves the manufacturing of a single tank, all environmental impacts associated with the mandrel and molds are fully allocated to the production phase.
    - **Cradle-to-grave LCA**: Under the assumption of full-scale industrial production, mandrel and molds are assumed to have a service life of 100 production cycles. Accordingly, only 1% (0.01) of their total environmental impact is attributed to the production of a single tank.

7.2 Inventory related to the production of the tanks

Important data related to the life cycle inventory is summarised in Table 1, Table 2 and Table 3. Table 1 presents the material consumption associated with the manufacturing of both tanks. Due to the larger surface area of the baseline tank, the steel required for mandrel production is correspondingly higher. However, the COCOLIH2T tank requires more material for the inner tank, as its design necessitates a thicker wall to compensate for a less favourable stress distribution compared to the axially symmetric cylindrical and spherical-end configuration of the baseline tank. For components such as the super-mold, mold, and outer vessel, where the wall thickness is assumed to be identical for both tanks, material usage is primarily governed by surface area. Consequently, the baseline tank exhibits higher material consumption in these components due to its larger surface area.

The production of prepreg sheets or tapes from dry fibres and resin involves significant energy consumption, which varies depending on the type of resin system used. Different resin systems have distinct processing requirements, leading to variations in energy demand. The energy consumption values adopted in this study for the production of prepregs using thermoset and thermoplastic resins are presented in Table 2, together with the references from which the data was obtained.

Table 1 Material requirements for the different components of COCOLIH2T and baseline tank

Material consumption in COCOLIH2T tank	
Part	***Material used***
Steel (Mandrel)	400.35 kg
CF/PAEK (Inner vessel)	91 kg
MDF (Super-mold)	1.70 m^3
CF/Epoxy (Mold)	136.20 kg
CF/Epoxy (Outer vessel)	65.37 kg
Material consumption in baseline tank	
Part	***Material used***
Steel (Mandrel)	543.22 kg
CF/Epoxy (Inner vessel)	55.93 kg
MDF (Super-mold)	1.79 m^3
CF/Epoxy (Mold)	152.94 kg
CF/Epoxy (Outer vessel)	72.84 kg

Table 2 Energy consumption for prepreg production from carbon fibres and resin as raw materials

Type of resin	*Energy consumption (MJ/kg)*	*Reference*
Thermoset (Epoxy)	40.0	[41]
Thermoplastic (PAEK)	25.1	[42,43]

Table 3 presents the energy consumption associated with the various manufacturing practices used in the production of the tanks. The table also includes references for the data sources. In the case of autoclave curing, studies have shown that energy consumption is primarily influenced by the size of the autoclave and the specific process parameters employed, rather than the mass of the material being cured [44]. Therefore, unlike other manufacturing techniques where energy use is expressed per kilogram of material, the energy consumption for autoclave curing is reported as an absolute value.

Table 3 Energy consumption for various manufacturing practices

Manufacturing technique	*Energy consumption*	*Reference*
AFP manufacturing	17.80 kWh/kg	[45]
Filament winding	0.75 kWh/kg	[41]
Hand layup	1.44 kWh/kg	[46]
Autoclave curing	17.60 kWh	[44]

While modelling the production of materials using the Ecoinvent database, efforts were made to incorporate region-specific datasets wherever available. The manufacturing and assembly of the tanks is done in Italy. Accordingly, the *market* activity for the production of materials in the Ecoinvent database are selected with a preference for geographical relevance. Priority was given to *market* dataset specific to Italy *('IT')*, followed by regional datasets such as *'Europe without Switzerland'* or Europe *('RER')*. In cases where only existing dataset for a *market* activity is *'global'* dataset, but, a region-specific dataset exist for the corresponding *production* activity, the latter is preferred in order to maintain geographical relevance and consistency.

7.3 Inventory related to the end-of-life of the tank components

This section describes the life cycle inventory of the EoL treatment of the tank components. As highlighted earlier, two EoL pathways are considered in the analysis, landfilling for Scenario-1, whereas incineration and recycling for Scenario-2. Inventory data sourced for these EoL pathways is presented in the following sections.

7.3.1 Landfilling

For both thermoset and thermoplastic CFRP waste, landfilling is modelled using the Ecoinvent dataset for mixed plastics disposed in a sanitary landfill. This dataset accounts for landfill construction, operational emissions, wastewater treatment, and long-term emissions associated with waste degradation.

For MDF, no dedicated EoL dataset is available in Ecoinvent. Therefore, fiberboard is selected as the closest proxy to represent MDF. In this dataset, fiberboard is assumed to be composed of wood and polyurethane (PU) in a ratio of 92.5% and 7.5% by weight, respectively. To model the landfilling of MDF, corresponding datasets for the landfilling of waste wood and waste PU as inert materials in sanitary landfills, as available in Ecoinvent database, are used, following the aforementioned composition ratio.

Landfilling of steel waste is also modelled using the available process in the Ecoinvent dataset for the treatment of scrap steel in an inert material landfill. As steel is treated as an inert material in this context, no direct emissions from degradation are considered. However, the dataset includes process-specific burdens such as land use and infrastructure construction allocated to the landfilled steel mass.

7.3.2 Incineration with energy recovery

For incineration of thermoset CFRPs, the study considers the data for the municipal incineration of mixed plastics, available in Ecoinvent database, for the modelling. This dataset includes emissions from the incineration process as well as the treatment of residual by-products. As per the *process* description, the incineration results in net recovery of 3.92 MJ of electricity and 7.66 MJ of thermal energy, for processing per kg of the plastic. These energy outputs are modelled as *avoided products* in OpenLCA, providing environmental credits to the system by avoiding burdens of production of electrical and heat energy via conventional means.

Table 4 Energy recovered during the incineration

Municipal incineration of	Electric Energy (MJ/kg)	Thermal Energy (MJ/kg)
CF/Epoxy	3.92	7.66
Waste PU	3.93	7.68
Waste Wood	1.74	3.49

In contrast to many studies reported in the literature [47–50], a conservative modelling approach is adopted in this work. Only the polymer matrix fraction of CFRP waste is assumed to undergo combustion and contribute to energy recovery. Carbon fibers are assumed to be inert during incineration and therefore do not contribute to energy generation. For the thermoset CFRP considered in this study, the matrix component in the composite is 35% by weight. Consequently, only 0.35 kg of material per kilogram of CFRP waste is assumed to contribute to energy recovery, while the full 1 kg is processed through the incineration facility. This assumption results in lower energy credits compared to those reported in many previous studies and is therefore considered conservative.

For incineration of MDF, consistent with the assumed composition in landfilling, i.e., 92.5% wood and 7.5% PU, separate datasets for municipal incineration of waste wood and waste PU, available in the Ecoinvent dataset, are used. The resulting electricity and thermal energy recovered from incineration is reported in Table 4, and is modelled as avoided products. MDF volumes reported in the inventory for the production phase are converted to mass using a density of 700 kg/m³.

7.3.3 Recycling

For recycling of thermoplastic CFRP components, mechanical recycling is considered in this study. In this process, laminated composite parts with continuous fibre reinforcement are shredded and converted into short-fibre-reinforced pellets. Due to the loss of fibre length and associated mechanical performance, the recycled material cannot be reused for the same high-performance application. As a result, a downcycling approach is assumed.

To account for this quality degradation, a conservative replacement ratio of 25% (by weight) is applied. Accordingly, the recycled material is assumed to replace only 25% of virgin CF/PAEK prepreg, which is modelled as an *avoided product*.

Energy consumption associated with the shredding process during recycling is explicitly included and modelled as 0.27 MJ/kg of thermoplastic CFRP waste, based on values reported in the literature [42,51].

In the case of steel, the production process is considered within the analysis is based on the electric arc furnace (EAF) method, which is a secondary steel production route. This means that steel is produced from iron scrap rather than from iron ore or pig iron. Since the iron scrap used in this process comes from a cut-off database, it is available for steel production without imposing any additional environmental burden. Consequently, the waste steel generated at the end of life of the mandrel is, in effect, already accounted for as recycled within the system. The only additional environmental impacts associated with recycling this steel arise from the sorting and pressing of the waste steel to convert it into usable iron scrap for production, which are added in the treatment process of the waste steel.

Detailed assumptions, calculations, references and other supporting information for all data presented here are provided in the provided supplementary material.

8 Impact Analysis – Production Phase

This section details the results of the LCA conducted for the production phase of the tank lifecycle and presents the valuable insights about the environmental impact of both tank configurations.

8.1 Thermoplastic versus thermoset

A major difference in the COCOLIH2T tank compared to the baseline tank is the change in the material from thermoset to thermoplastic resin, specifically, from CF/Epoxy to CF/PAEK. It is essential to first compare the environmental impact of both material systems. The key difference in the material systems is due to the change in resin; however, minor variations in carbon fibre content by weight (1.5% higher in CF/PAEK compared to CF/Epoxy), also contribute slightly.

An LCA study is conducted to compare the environmental impact for the production of 1 kg of each material and the results are presented in Figure 10. The impact categories are arranged in the descending order. Results are presented in the form of percentage change and are included for all eighteen impact categories defined in the ReCiPe impact assessment method. The percentage change is calculated relative to CF/Epoxy, indicating the impact of switching from a thermoset to a thermoplastic matrix.

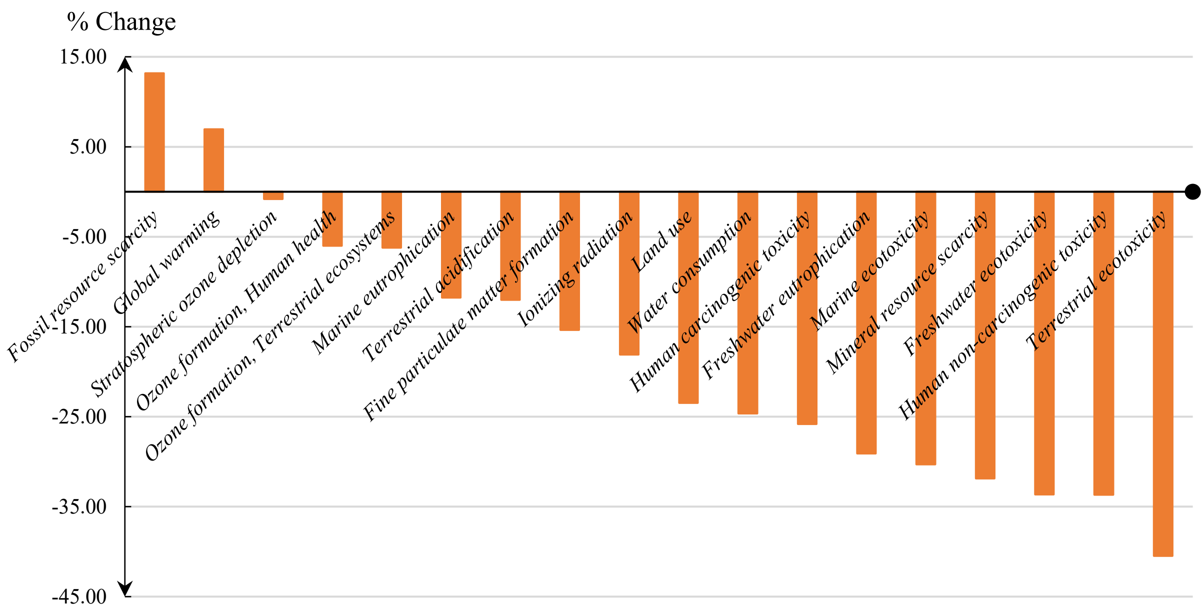

Figure 10 Percentage change in the environmental impact for each impact category when transitioning from the thermosets (CF/Epoxy) to the thermoplastics (CF/PAEK). Positive values indicate increased emissions, whereas, negative values indicate a reduced impact.

The analysis shows that CF/PAEK outperforms CF/Epoxy in all but two environmental impact categories, *fossil resource scarcity* and *global warming*. In all other categories, the thermoplastic composite demonstrates a significantly lower environmental burden, supporting the transition from CF/Epoxy to CF/PAEK. Furthermore, this study focuses solely on the production stage and does not account for end-of-life considerations. Given that thermoplastics are recyclable and potentially reusable, it is anticipated that incorporating end-of-life analysis would further strengthen the case for CF/PAEK.

8.2 COCOLIH2T tank versus baseline tank

The results of the life cycle assessment were calculated for all the impact categories for both the baseline and COCOLIH2T tank. The percentage change in the environmental impact when transitioning from the baseline tank to COCOLIH2T tank is presented in Figure 11. The impact categories are arranged in descending order of their influence, with the first eleven categories showing a positive percentage change, indicating that the COCOLIH2T tank resulted in higher emissions compared to the baseline tank. In contrast, the remaining seven categories show a negative percentage change, suggesting that the COCOLIH2T tank performs better in these areas.

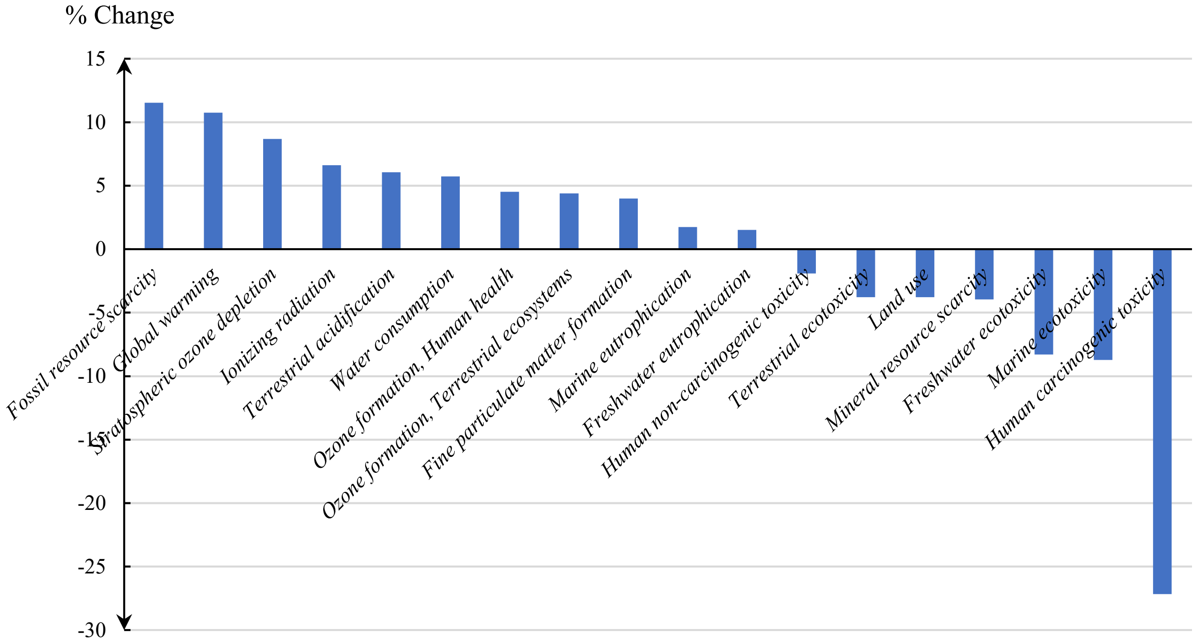

Figure 11 Percentage change in the environmental impact for each impact category when transitioning from the baseline tank to the COCOLIH2T tank. Positive values indicate increased emissions, whereas, negative values indicate a reduced impact.

The most significant improvement is observed in the *human carcinogenic toxicity* category, where emissions are reduced by 24.9%. This reduction is attributed to the increased use of steel in the baseline tank. Inventory analysis reveals that the baseline tank consumes 142.87 kg more steel than the COCOLIH2T tank, which is a major contributing factor to its higher impact in this category. On the other hand, the COCOLIH2T tank results in higher impact in the *Fossil Fuel Scarcity* and *Global Warming* categories, both exceeding a 10% increase. For all other impact categories, the percentage change, whether positive or negative, remains within a 10% range. These results suggest that no clear conclusion can be drawn regarding which tank is more environmentally friendly overall, as each has its strengths and drawbacks across different impact categories.

8.3 Normalized impact assessment score for the tanks

A direct comparison of the absolute impact assessment values does not provide a good insight, as the categories differ in both units and scales. Without normalization, it is difficult to discern which environmental impacts are relatively more significant and which are negligible. Therefore, normalization is necessary to contextualise the results. In this study, normalization factors provided by the ReCiPe impact assessment method are applied. These factors represent the annual global average emissions per person for each impact category, allowing for the comparison of different environmental effects on a common scale.

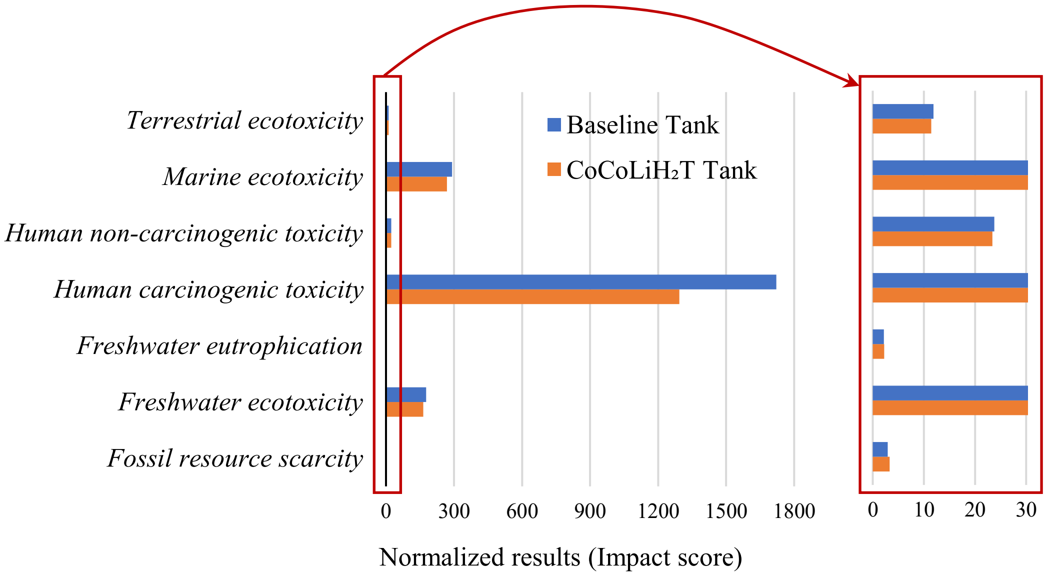

Figure 12 Normalized environmental impact scores for the baseline and COCOLIH2T tank (Only the impact categories with normalized score greater than 1.5 are included.)

After normalization, the majority of the impact categories, eleven out of eighteen to be exact, exhibit a normalized score below 1.5, indicating a relatively low contribution to overall environmental cost. The normalized scores of other seven impact categories are shown in Figure 12. The most significant categories with higher normalized scores turn out to be *human carcinogenic toxicity*, *marine ecotoxicity*, and *freshwater ecotoxicity*. Interestingly, these as well as most of the other categories appearing among these seven prominent impact categories, are the ones where the COCOLIH2T tank outperforms the baseline design. Based on these normalized results and their alignment with global average emissions, it can be concluded that the COCOLIH2T tank holds a relative environmental advantage over the baseline configuration in the most critical impact areas.

8.4 Component level contributions to the environmental impact

To identify the primary contributors to the overall environmental impact of the tanks, a component-level analysis was conducted. Both the baseline and COCOLIH2T tanks consist of two vessels, an inner and an outer vessel. For the baseline tank, the inner vessel is manufactured using FW, involving two main components, the mandrel and the vessel itself. In the case of the COCOLIH2T tank, the inner vessel is produced using AFP, also involving a mandrel and the vessel. Whereas, the outer vessel in both tanks is fabricated via a hand lay-up process, utilizing a CF/Epoxy mold, and this mold is created using an MDF super-mold. Therefore, the outer vessel involves three components, the MDF super-mold, the CF/Epoxy mold, and the outer vessel itself.

To quantify each component's overall contribution to environmental impact, the percentage contribution of each component was first individually calculated for all eighteen ReCiPe impact categories. Then, an overall average contribution is obtained for that component by averaging across all the impact categories. This procedure was applied to both the baseline and COCOLIH2T tank. A summary of the method is provided in Table 5. While this method simplifies certain nuances, it offers a representative understanding of component-level contributions. The results thus obtained are presented in Figure 13.

Table 5 Representative table to showcase the methodology for calculating total percentage contribution of individual components to overall environmental impact

Impact Categories	Baseline Tank Manufacturing					
	Inner Vessel		Outer Vessel			
	Mandrel	Vessel	MDF Super-mold	CF/Epoxy Mold	Vessel	
Fine particulate matter formation	6.18	13.74	23.36	38.59	18.13	$\Sigma\,(row) = 100$
Fossil resource scarcity	2.36	16.23	14.95	45.13	21.33	
…	-	-	-	-	-	
⋮						
Average contribution	$\Sigma\,(column)/18$	$\Sigma\,(column)/18$	$\Sigma\,(column)/18$	$\Sigma\,(column)/18$	$\Sigma\,(column)/18$	

Full data tables are omitted from the report for brevity. Though, there were a few key insights gained from the results. As expected, contribution towards *human carcinogenic toxicity* is overwhelmingly (greater than 90%) attributed to the mandrel, primarily due to the high impact of steel production. For the category of *land use*, over 90% of the impact arises from the MDF super-mold in both tanks, as MDF production relies heavily on raw wood resources.

Figure 13 shows the average percentage contribution for each component in both the baseline and COCOLIH2T tank. The most significant impact contributor is the outer vessel manufacturing, accounting for 73.63% and 66.11% of the total environmental burden for the baseline and COCOLIH2T tanks, respectively, in their respective production. Within this category, the MDF super-mold and

CF/Epoxy mold dominate, while the vessel material and manufacturing itself contributes relatively little. It is important to note that this analysis considers only the manufacturing stage at laboratory scale, i.e., the manufacturing of one tank. In real-world production, the molds would be reused across multiple manufacturing cycles, significantly reducing their per-unit contribution. This aspect is addressed in the cradle-to-grave analysis presented below in sections 7.5 and 8.5.

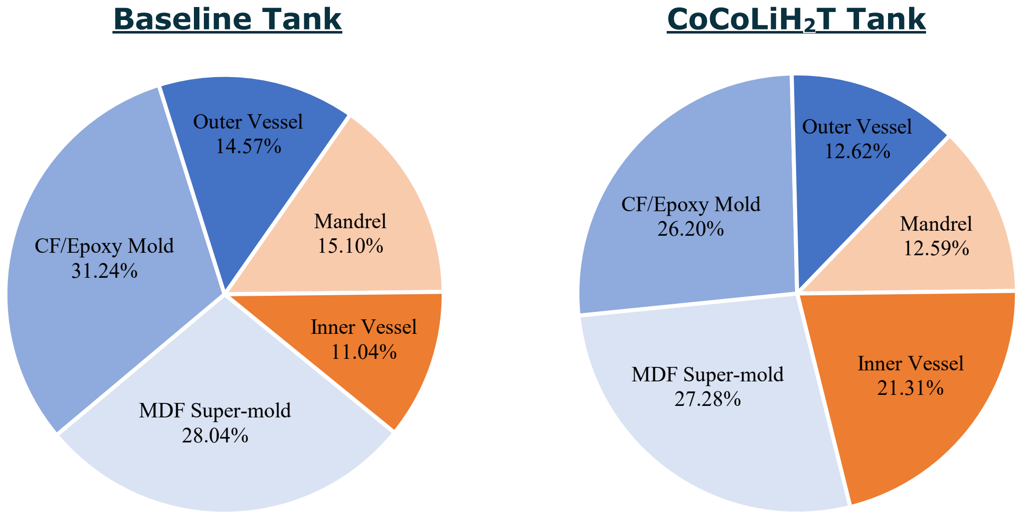

Figure 13 Total percentage contribution to the environmental impact from the production of each component of the baseline and COCOLIH2T tanks

Another noteworthy observation is that the inner vessel contributes a higher percentage to the total impact in the COCOLIH2T tank compared to the baseline. As discussed earlier, although thermoplastics like CF/PAEK offer better environmental performance than thermosets like CF/Epoxy, the increased impact observed here can be attributed to the larger amount of material used for the inner vessel in the COCOLIH2T tank. In addition, the inner vessel of the COCOLIH2T tank is manufactured using AFP, which is significantly more energy-intensive than FW, which is being reflected in the results. Finally, the higher relative contribution may also be influenced by reduced impacts from other components in the COCOLIH2T design, thereby increasing the proportional contribution of the inner vessel.

8.5 Evaluation of mold or mandrel material choices

As observed in the previous section, the molds used in outer vessel manufacturing contribute significantly to the overall environmental impact. Additionally, steel used in the mandrels also showed a high impact particularly in the *human carcinogenic toxicity* category. Given this impact, it becomes essential to explore whether alternative mold or mandrel materials could reduce these environmental burdens. This analysis evaluates environmental performance of MDF and aluminium in comparison to steel. For MDF, a density of 700 kg/m^3 is assumed to conduct the analysis. For aluminium, both cast aluminium and wrought aluminium variants are included to reflect typical industrial options.

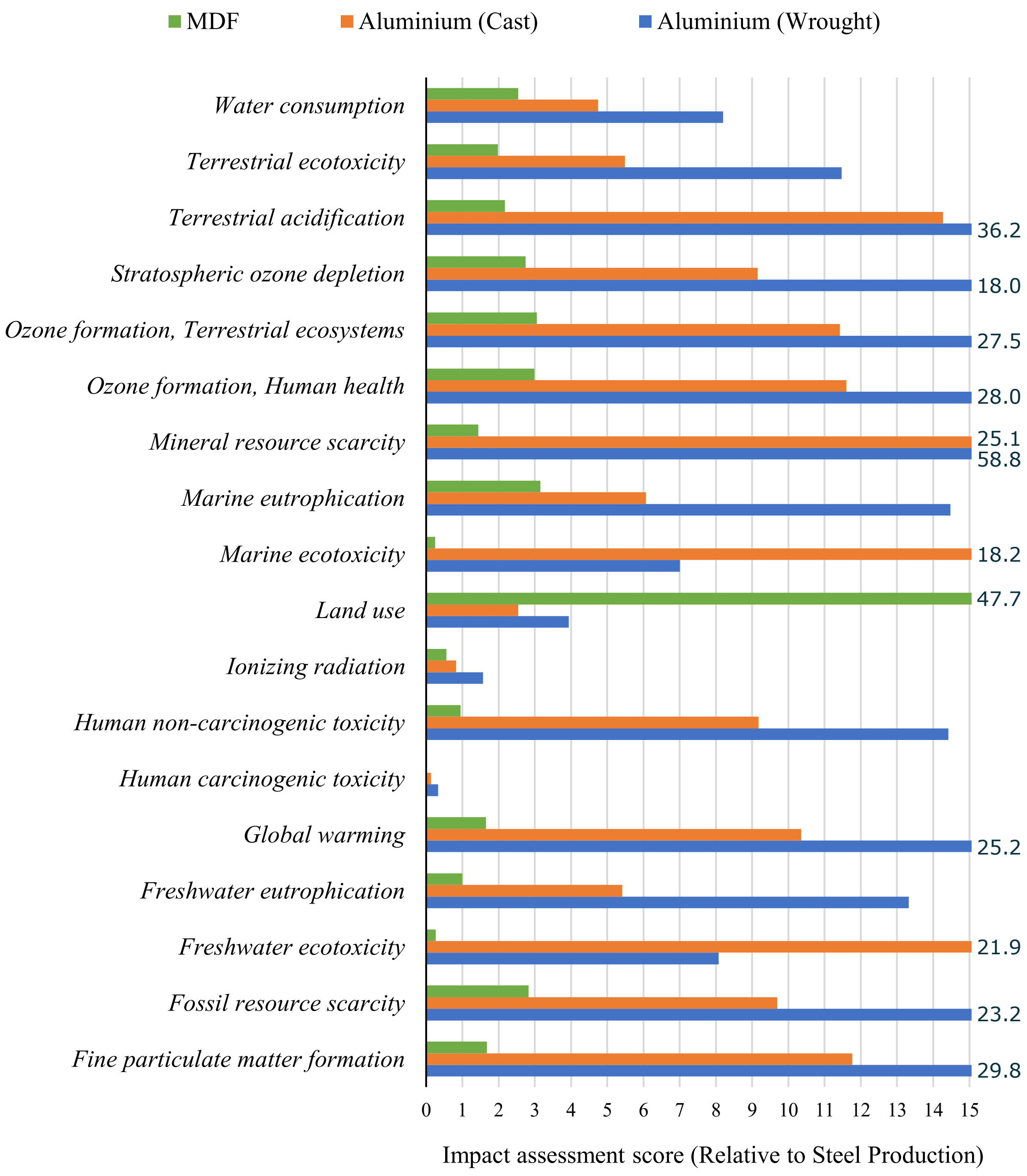

Figure 14 Environmental impacts of 1 kg of MDF, aluminium (cast), and aluminium (wrought) relative to those of steel.

The impact assessment results, based on the modelling of 1 kg of each of the four materials, are presented in the form of a bar chart in Figure 14 . The results are shown relative to those of steel, thus, a value of '*2*' indicates twice the emissions compared to the production of 1 kg of steel. Horizontal axis of the bar chart is truncated at the value of '*15*', to highlight emissions closer to steel's level, i.e., value near to *'1'*. For the bars exceeding this range, the exact values are provided to the right of the chart.

MDF and both types of aluminium show lower impacts than steel in the category of *human carcinogenic toxicity*. However, aluminium exhibits extremely high impacts in most categories. It is most notable in *mineral resource scarcity*, where it can exceed steel's impact by over 50 times in wrought form and over 25 times in cast form. This makes aluminium an unsuitable alternative. One reason for these significantly higher values compared to steel emissions is the production method modelled for steel in the analysis. The steel production considered in this study is based on the electric arc furnace process, which is more energy-efficient and less carbon-intensive compared to the less efficient means to produce steel using the basic oxygen furnace converter process.

Another important observation is the difference in environmental impact between cast and wrought aluminium. Typically, wrought aluminium is expected to have a higher footprint due to increased processing, but not double that of cast aluminium as seen in these results. The difference would normally be minimal and mainly be attributed to higher energy demand. Upon closer examination of the modelling, it was found that the Ecoinvent database distinguishes cast and wrought aluminium not by energy consumption during production or transformation of aluminium ingots, but by the proportion of recycled scrap versus primary ingot material used. For cast aluminium, approximately 75% is sourced from scrap (either new scrap or post-consumer), with only 25% coming from primary ingots. In contrast, wrought aluminium contains only about 40% scrap and 60% primary ingot, more than double the share of primary aluminium compared to cast. This distinction makes sense because wrought aluminium requires superior mechanical properties and lower impurity tolerance, necessitating a higher proportion of new aluminium. Since producing primary ingots from ore is an environmentally intensive process, this explains why wrought aluminium has nearly double the environmental impact compared to cast aluminium in most of the categories.

MDF offers some environmental advantages in a few additional categories, such as *freshwater ecotoxicity*, *ionizing radiation* and *marine ecotoxicity*, but its performance is inconsistent, and it carries significant burdens in categories such as *land use*. Overall, despite its drawbacks, steel emerges as the most balanced and environmentally favourable option among these four, when considering performance across all eighteen ReCiPe impact categories.

8.6 Closure

The results for the environmental assessment of the production phase indicate that between baseline and COCOLIH2T tank, there is no single environmentally superior design which proves to be better across all impact categories. Though, after normalizing the results to global per capita averages, three impact categories *human carcinogenic toxicity*, *marine ecotoxicity*, and *freshwater ecotoxicity*, emerged as particularly relevant and were the top contributors for environmental damage. In all three categories, the impact scores were substantially lower for the COCOLIH2T tank. This suggested a notable environmental superiority of the COCOLIH2T tank over the baseline tank design.

Importantly, the analysis also revealed that the major environmental burdens in the tank manufacturing process do not stem from the vessel materials themselves, but from the production of the mold, particularly those made from MDF and CF/Epoxy. Comparing materials for their environmental impact indicated that replacing CF/Epoxy with CF/PAEK (a thermoplastic) could yield significant environmental benefits. Similarly, replacing the MDF mold with steel offers advantages in most categories, although steel was found to have a higher impact in *human carcinogenic toxicity*, *marine ecotoxicity* and *freshwater ecotoxicity*.

9 Impact analysis – Cradle-to-grave

This section presents the results of the LCA conducted over the full life cycle of the tanks, encompassing a cradle-to-grave system boundary. It provides key insights into the environmental impacts of both tank configurations and impact of EoL pathways on it.

9.1 Comparison of thermoplastics and thermoset

One of the major distinctions between the two tank designs is the use of thermoplastic composites in the COCOLIH2T tank, which are expected to exhibit a lower environmental impact than thermoset composites, primarily due to their recyclability. In a previous chapter, a life cycle assessment of the production phase was conducted for 1 kg each of thermoset (CF/Epoxy) and thermoplastic (CF/PAEK) composites. That analysis showed that thermoplastic composites performed better in 16 out of 18 impact categories, exhibiting a lower environmental burden than their thermoset counterparts.

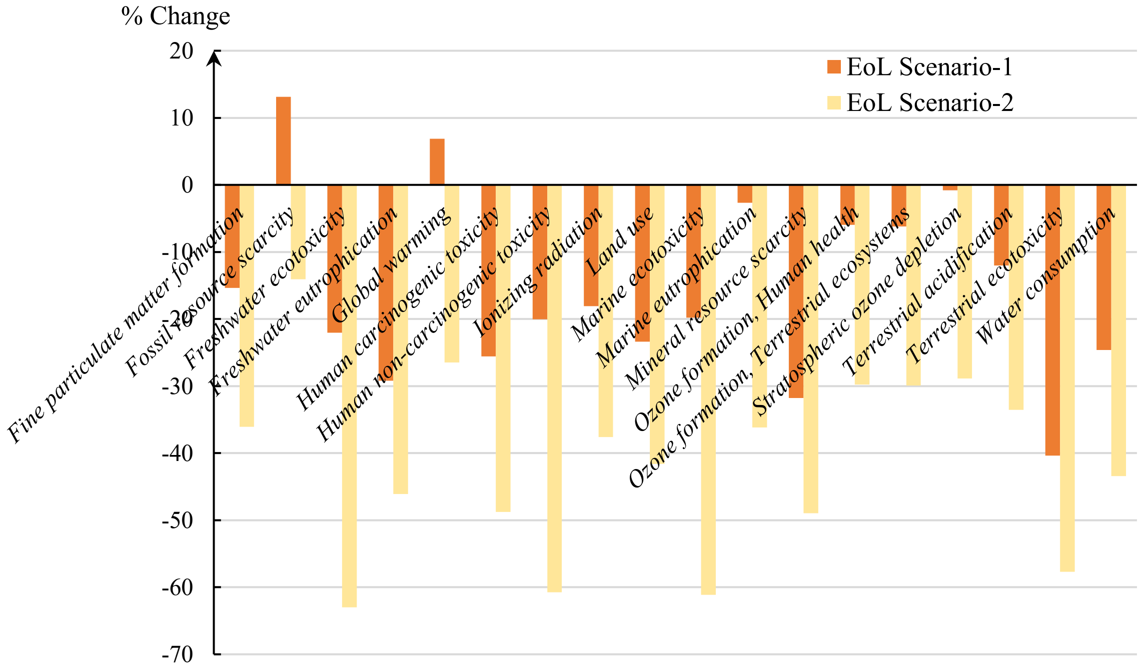

Figure 15 Percentage change in the environmental impact when transitioning from thermoset (CF/Epoxy) material to thermoplastic (CF/PAEK) material. (A negative value indicate lower emissions in case of thermoplastics and vice-versa)

In the present study, the comparison is extended by including the EoL scenarios. For modelling purposes, the production of 1 kg of prepreg is considered for both thermoset and thermoplastic composites, followed by treatment of the same amount as waste at EoL. The manufacturing of composite parts is intentionally excluded to isolate the environmental impacts associated solely with the material systems and avoid any effects from manufacturing process-specific variations.

The results are presented as percentage changes relative to the CF/Epoxy and are illustrated in Figure 15. Negative values indicate a reduction in environmental impact when switching from thermoset to thermoplastic composites. For EoL Scenario-1, i.e. landfilling, results obtained closely align with the results obtained for the production phase (Figure 10). Since both materials are disposed of as mixed plastic waste, their EoL emissions are identical. Consequently, the EoL stage introduces only a constant offset to the production-related impacts, altering the percentage change, but not the overall interpretation of the results.

In contrast, when recycling is considered (EoL Scenario-2), thermoplastic composites outperform thermosets across all impact categories, with reductions of at least 14% in all categories and exceeding 60% in a few of them. These findings indicate that, for an equal mass, thermoplastic composites offer a substantially lower environmental impact than thermoset composites, suggesting the idea that CFRP industry can be benefitted by transitioning toward thermoplastic-based systems.

9.2 Comparison of the tank designs based on the impact assessment

A comparative impact assessment across all eighteen environmental categories for both EoL scenarios is presented in Figure 16. The results are expressed as the percentage change in emissions when transitioning from the baseline tank to the COCOLIH2T tank. Positive values indicate an increase in emissions, whereas negative values indicate a reduction.

The results indicate that, except for the category of *human carcinogenic toxicity* in EoL Scenario-2, all other cases exhibit a positive percentage change, implying that the COCOLIH2T tank is associated with a higher life-cycle environmental impacts compared to the baseline tank. At first glance, these findings appear to contradict the results presented for the production-phase, where COCOLIH2T tank performed better than the baseline tank for certain impact categories (Figure 11).

To recall, in the LCA study of the production phase, a laboratory-scale production setup was assumed, in which all the emissions related to mandrel and mold production were allocated towards the production of a single tank. In contrast, the present analysis assumes commercial-scale manufacturing, where the environmental burdens of mandrel and molds are distributed over 100 production cycles. Consequently, while the results of the production-phase reflected the additional material (e.g., MDF, steel, and CF/epoxy) consumption in case of baseline tank for mandrel and mold fabrication, these contributions are no longer as influential in the current assessment.

In the present analysis, the primary contributors of the environmental impacts are inner and outer vessels of the tanks (as discussed further in Section 4.5). Examination of life cycle inventory data reveals that the COCOLIH2T tank consumes a significantly larger quantity of material (~1.6 times more in weight) for the inner vessel compared to the baseline tank. Moreover, the inner vessel of the COCOLIH2T tank is manufactured using AFP, which is approximately 24 times more energy-intensive (based on per kg of material fabricated) than filament winding, the method employed for the manufacturing of inner vessel of baseline tank. The combined effect of increased material usage and higher energy consumption outweighs the environmental benefits associated with the use of thermoplastics instead of thermosets, resulting in higher overall emissions for the COCOLIH2T tank. Even for *human carcinogenic toxicity*, where COCOLIH2T tank performs better under the EoL Scenario-2 assumption, the magnitude of this reduction is small, with only 1.79% lower than the baseline tank.

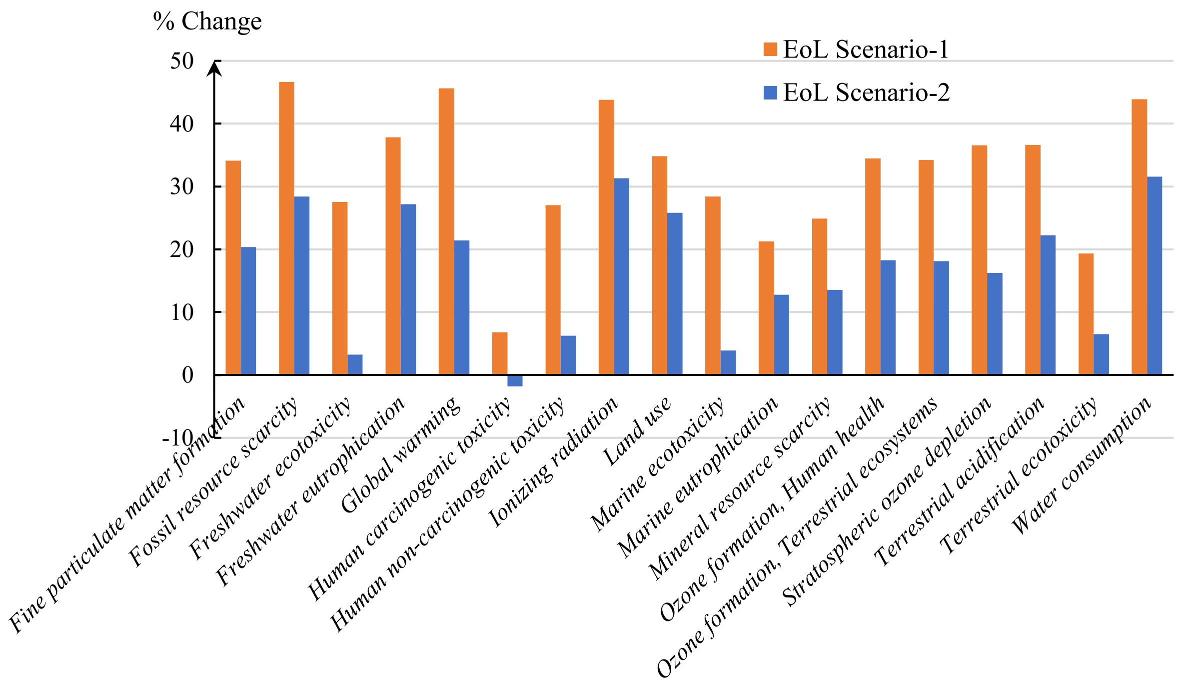

Figure 16 Percentage change in the environmental impact when transitioning from baseline tank to the COCOLIH2T tank, for both end-of-life strategies considered. (A positive value indicate higher emissions in case of COCOLIH2T tank and vice-versa)

Importantly, this analysis highlights how sensitive LCA outcomes are to underlying assumptions, emphasizing the need for careful scrutiny of such assumptions when using LCA results to inform policy decisions or design optimization.

Focusing on the results of EoL Scenario-1 in Figure 11, the percentage change in emissions when transitioning from the baseline tank to the COCOLIH2T tank is always higher than the change observed for EoL Scenario-2. This indicates that the COCOLIH2T tank performs substantially worse if all materials are landfilled at the end of their life. Under incineration and recycling case (EoL Scenario-2), the COCOLIH2T tank gains environmental credits arising from the recycling of CF/PAEK and energy recovery from incineration of CF/Epoxy, which partially offset the emissions. However, comparatively, the baseline tank does not benefit from such recycling credits and hence, the difference between the two tanks is less pronounced in the EoL Scenario-2.

9.3 Comparison of the tank designs based on normalized impact score

A direct comparison of absolute impact assessment values offers limited insight because impact categories differ substantially in units and scale. Consequently, it is difficult to identify relatively significant environmental burdens without normalizing the results based on a common basis. To address this, normalization is applied to contextualise the results across categories. In this study, normalization factors from the ReCiPe impact assessment method are used. These factors represent annual global average emissions per capita for each impact category, enabling meaningful cross-category comparisons.

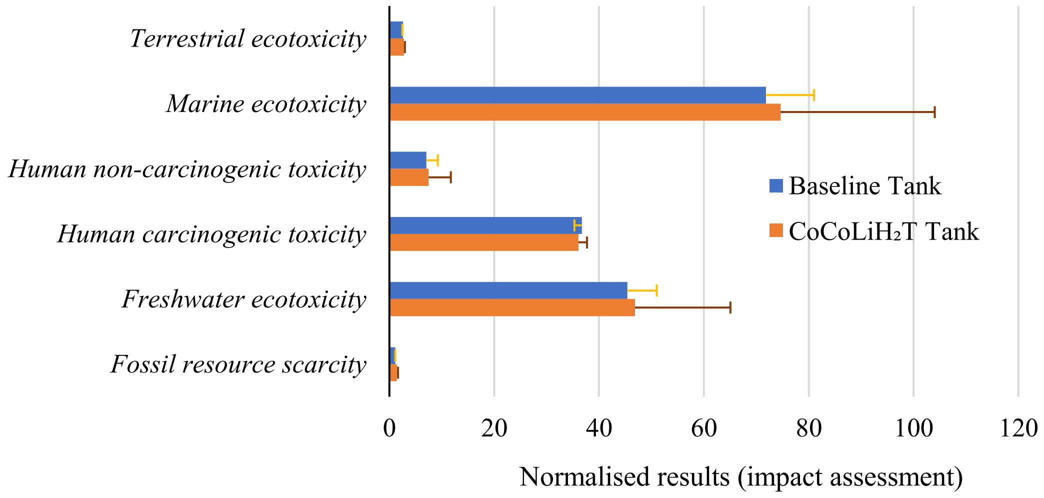

Figure 17 Normalized environmental impact scores for the baseline and COCOLIH2T tank. Bars represent the impact score for the EoL Scenario-2 (incineration and recycling), whereas error bars represent the score for the EoL Scenerio-1 (landfilling). Only categories with impact score more than 1 are included.

Figure 17 presents the normalized impact scores for the EoL Scenario-2, for both the baseline tank and the COCOLIH2T tank. Only impact categories with normalized scores greater than 1 are shown in the figure. Error bars represent the impact scores for the EoL Scenario-1, thereby capturing the range of potential emissions associated with different EoL strategies. Out of the eighteen, six impact categories emerge as particularly influential: *terrestrial ecotoxicity*, *marine ecotoxicity*, *human non-carcinogenic toxicity*, *human carcinogenic toxicity*, *freshwater ecotoxicity*, and *fossil resource scarcity*. Notice from Figure 16, the first five of these six categories exhibit lowest values (less than 7% change) for EoL Scenario-2, indicating a relatively smaller difference in environmental impact of both the tanks. The same can also be observed from Figure 17, where the differences in normalized impact scores of both the tanks are relatively small, with a maximum difference in the impact scores of 2.81 points, observed for *marine ecotoxicity*. This suggests that under incineration and recycling EoL conditions, both tank designs exhibit comparable environmental performance across the dominant impact categories. Among these, the COCOLIH2T tank performs slightly better in the category of *human carcinogenic toxicity*.

However, when the focus shifts to the EoL Scenario-1, i.e., error bars presented in the chart, the differences between the two tank designs become more pronounced. In case of *marine ecotoxicity*, a difference of 23.04 points is observed and in case of *freshwater ecotoxicity* the difference lies at 14.05 points. Even if for remaining three categories the values are on the lower side, they are still higher than the difference observed in case of EoL Scenario-2. These results once again indicate that while the COCOLIH2T tank can achieve environmental impacts comparable to the baseline tank under optimal EoL strategies, its performance deteriorates significantly under landfill-dominated EoL scenarios.

Another interesting observation gained from the Figure 17 is that in case of the baseline tank, the impact score is higher for EoL Scenerio-2 compared to Scenario-1 in impact categories of *terrestrial ecotoxicity* and *human carcinogenic toxicity*, highlighting that in some cases, landfilling can outperform the supposedly better EoL strategy of incineration with energy recovery and recycling. This is further discussed in detail in the next section.

Table 6 Largest and second-largest contributing flows towards the environment impact of the most-influential impact categories

Impact Category	Largest Contributor	Second-largest Contributor
Terrestrial ecotoxicity	Copper, to air (smelting of copper)	Vanadium, to air (electricity and heat generation from oil, waste plastic incineration)
Marine ecotoxicity	Copper, ion, to ground water (treatment of scrap copper, treatment of waste plastic)	Zinc, ion, to ground water (treatment of waste plastic, treatment of spoil from hard coal mining, treatment of spoil from lignite mining)
Human non-carcinogenic toxicity	Zinc, ion, to ground water (treatment of waste plastic, treatment of spoil from hard coal mining, treatment of spoil from lignite mining)	Arsenic, ion, to ground water (treatment of spoil from hard coal mining, treatment of spoil from lignite mining)
Human carcinogenic toxicity	Chromium VI, to ground water (treatment of electric arc furnace slag, treatment of spoils from hard coal mining)	Chromium VI, to surface water (treatment of electric arc furnace slag)
Freshwater ecotoxicity	Copper, ion, to ground water (treatment of scrap copper in electricity transmission, treatment of waste plastic)	Zinc, ion, to ground water (treatment of waste plastic, treatment of spoil from hard coal mining, treatment of spoil from lignite mining)
Fossil resource scarcity	Gas, natural, in ground (gas and petroleum production)	Energy, from gas, natural (PAN fibre production)

A more detailed analysis of the contributions to these most influential impact categories is presented in Table 6. The table reports the largest and second-largest elementary flows (i.e., direct emissions or resource extractions from nature) contributing to each impact category, together with the processes primarily responsible for these flows. Processes associated with copper are linked to electricity transmission infrastructure, while those related to coal, lignite, or natural gas correspond to energy production in the form of heat or electricity.

The results indicate that the dominant contributions can broadly be attributed to four main groups: (i) production and treatment of copper, (ii) steel production via electric arc furnace route, (iii) treatment of waste plastics, and (iv) conventional energy generation using fossil fuels such as oil, coal, and gas. As copper and steel are essential materials for electrical infrastructure and manufacturing, respectively, mitigation options for processes related to these materials are comparatively limited. In contrast, the latter two offer more direct opportunities for impact reduction.

Impacts associated with energy generation could be significantly reduced by replacing conventional fossil fuel based energy sources with renewable alternatives, thereby lowering emissions across multiple impact categories. Similarly, improvements in plastic waste treatment, particularly through the development and scaling-up of effective recycling (or repurposing) technologies, could reduce emissions associated with their landfilling and incineration. Overall, the results highlight that transitioning to renewable energy systems and enhancing plastic recycling represent promising pathways for reducing impacts in the dominant impact categories identified in this study.

9.4 Comparison of the EoL strategies for their environmental performance

Previously, Figure 16 compared the environmental gains and losses associated with transitioning from the baseline tank to the COCOLIH2T tank under a given EoL strategy. In contrast, the present analysis reorganizes the same dataset to evaluate how environmental impacts change for a given tank design when transitioning from EoL Scenario-1 (landfilling) to EoL Scenario-2 (incineration with energy recovery and recycling). This perspective provides additional insights about the impacts EoL pathways have on the environment. It is important to note that the manufacturing and use-phase remain identical in both EoL scenarios for a given tank. Consequently, all observed differences arise exclusively from changes in the EoL treatment.

Normalized scores are used to present the results instead of the percentage change. Although, percentage changes in emissions can be a useful and convenient metric for comparing scenarios, they may sometimes be misleading. For instance, in the marine eutrophication category for the baseline tank, emissions decrease from 0.32 kg N eq. in EoL Scenario-1 to 0.07 kg N eq. (Nitrogen equivalent) in EoL Scenario-2, corresponding to a reduction exceeding 75%. While the relative change is numerically large, the absolute change remains small when compared to the per capita global average (normalization factor) of 4.61, which is one order of magnitude higher. Thus, the environmental relevance of the result may be overstated when expressed solely as percentage. Therefore, the discussion in this section is based on normalized scores. The impact categories showing a difference greater than 10^{-2} units (0.01) between the impact scores of both the EoL scenarios are examined here. For all other categories, the differences are considered sufficiently small to assume that changing the EoL scenario does not lead to any variation in environmental impact.

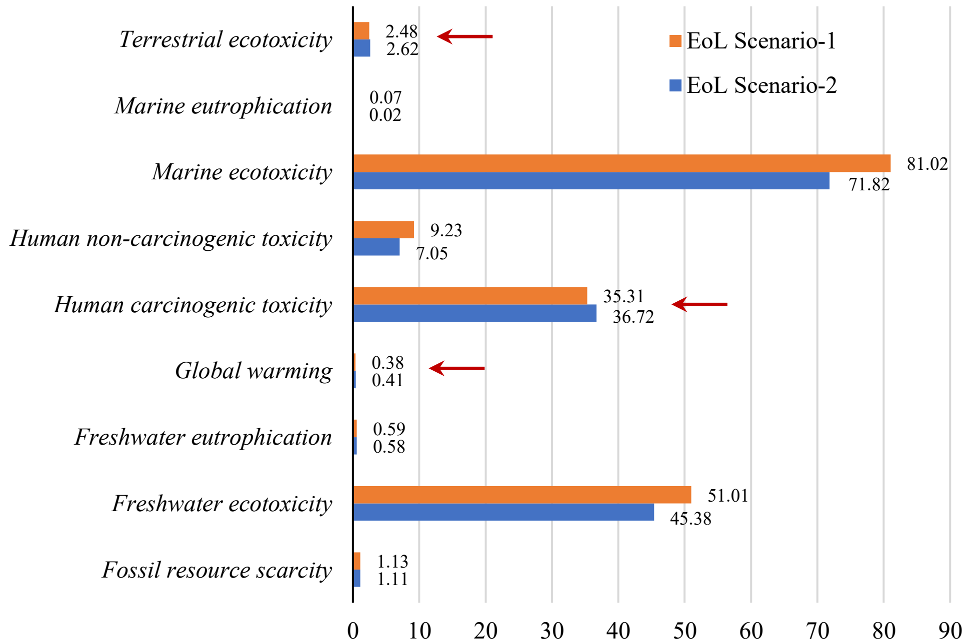

Figure 18 Comparison of emissions associated with different EoL scenarios for baseline tank. Results are presented as normalized scores, where, EoL Scenario-1 represents landfilling, and EoL Scenario-2 represents incineration and recycling.

9.4.1 Baseline tank

The results obtained for the baseline tank, are showcased in Figure 18. Nine impact categories out of eighteen showcased a difference of more than 10^{-2} units between the impact scores of both the EoL scenarios. Out of these nine, three categories, i.e., *terrestrial ecotoxicity*, *human carcinogenic toxicity*, and *global warming*, exhibit higher emissions under EoL Scenario-2 (incineration and recycling) compared to landfilling, which is a key and somewhat unexpected observation. These categories are highlighted with a red arrow in the figure. These categories, exhibit an increases of 8.33%, 5.50%, and 4.02%, respectively. Though the change is modest, this finding demonstrates that a transition away from landfilling is not universally beneficial across all impact categories.

Further investigation reveals that the increased impact in *global warming* in EoL Scenario-2 is primarily driven by CO_2 emissions released during incineration of waste plastic. In contrast, landfilling contributes to negligible amount of post-use emissions to this category. A similar explanation applies to *terrestrial ecotoxicity* and *human carcinogenic toxicity*, which show an increased impact in the incineration EoL pathway due to elevated emissions of vanadium and chromium VI, respectively, emissions that are largely absent in the landfilling pathway.

Conversely, other six categories in Figure 18 showcase a benefit for going for the EoL Scenario-2. Among these, *marine ecotoxicity*, *freshwater ecotoxicity* and *human non-carcinogenic toxicity* showcase a noticeable jump of 9.20, 5.63 and 2.18 points respectively, in their normalized scores. This significant reduction in the emissions provides meaningful support for incineration and recycling as an environmentally favourable EoL option for the baseline tank.

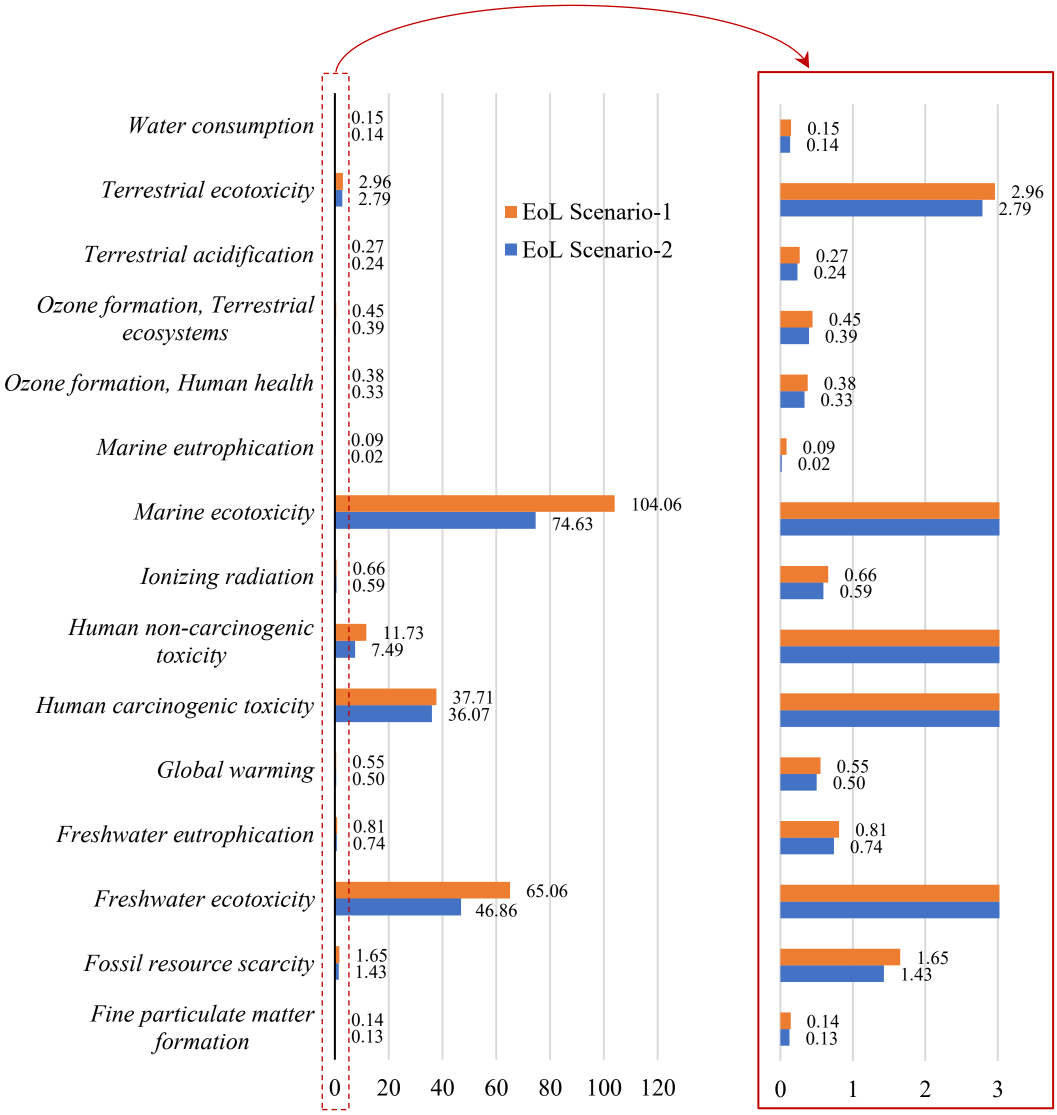

Figure 19 Comparison of emissions associated with different EoL scenarios for COCOLIH2T tank. Results are presented as normalized scores, where, EoL Scenario-1 represents landfilling, and EoL Scenario-2 represents incineration and recycling.

9.4.2 COCOLIH2T tank

The results obtained for the COCOLIH2T tank, are presented in Figure 19. Fifteen impact categories out of eighteen had a difference of more than 10^{-2} units between the impact scores of both the EoL scenarios, highlighting a change in emissions upon changing the EoL scenario. In contrast to the baseline design, the COCOLIH2T tank exhibits lower environmental impacts across all categories when transitioning to EoL Scenario-2. Notably, the categories that showed increased impacts for the baseline tank under incineration and recycling pathway do not exhibit such increases for the COCOLIH2T tank. Although incineration-related emissions are still present, they are more than compensated by the environmental credits associated with the recycling of CF/PAEK composites. Recycling avoids the production of virgin carbon fibre and PAEK, resulting in substantial avoided burdens that outweigh emissions from the incineration processes.

Among the impact categories, *marine ecotoxicity*, *freshwater ecotoxicity* and *human non-carcinogenic toxicity* once again show the largest reductions, with decreases of 29.43, 18.21 and 4.24 points in their normalized scores, respectively. These reductions are substantially greater than those observed for the baseline tank. Although both EoL scenarios contribute notably towards emissions, the differential treatment of waste plastic is a primary driver of the observed differences here. As shown in Table 6, waste plastic treatment is one of the main contributors to emissions across all three categories. In EoL Scenario-2 for COCOLIH2T tank, as plastic waste from the inner vessel is being recycled, there are no emissions associated with it for these impact categories, which leads to the reduction in emissions compared to EoL Scenario-1.

Overall, across the tank designs and EoL scenarios, recycling emerges as the most environmentally favourable EoL pathway, which aligns with expectations for a composite-intensive systems. However, the results also demonstrate that incineration with energy recovery is not universally superior to landfilling across all impact categories. Consequently, the optimal EoL route is context-dependent and should be determined based on regional conditions, temporal factors, and the impact categories deemed most critical, acknowledging that different pathways perform better across different environmental dimensions.

9.5 Contribution of individual tank component towards the environmental impact

As discussed earlier, each tank system consists of five components: the steel mandrel, inner vessel, MDF super-mold, CF/Epoxy mold, and outer vessel. This section examines the relative contribution of each component to the overall environmental impact in order to identify the dominant contributors. Because the mandrel and molds are reused over hundred tank production cycles, their environmental burdens per tank are substantially diluted. Consequently, their contributions are negligible relative to those of the inner and outer vessels. For clarity and relevance, the MDF super-mold and CF/Epoxy mold are therefore combined into a single category (“mold”), as their individual contributions are too small (even less than 1% of total impact in many categories) to yield meaningful insights when treated separately.

9.5.1 Baseline tank

For the baseline tank, the percentage contribution of the four considered components (inner vessel, outer vessel, mandrel, and mold) is broadly consistent across both EoL scenarios. On average, approximately 40% of the total impact originates from the inner vessel, about 53% from the outer vessel, and the remaining ~7% from the mandrel and mold combined, with the mold contributing more than the mandrel. Higher contributions of outer vessel here can be attributed to its higher weight. For most impact categories, this average distribution is representative, with only minor variations of less than ± 5% in the relative contributions of the inner and outer vessels. The exact values obtained for average contributions across all categories and EoL scenarios are presented in Figure 20. The figure also highlights the percentage contribution from the material usage and from the manufacturing, for both inner and outer vessel. It can be observed that the contribution from the energy consumption during manufacturing is rather negligible and material (thermoset) consumption is the major contributor of the emissions.

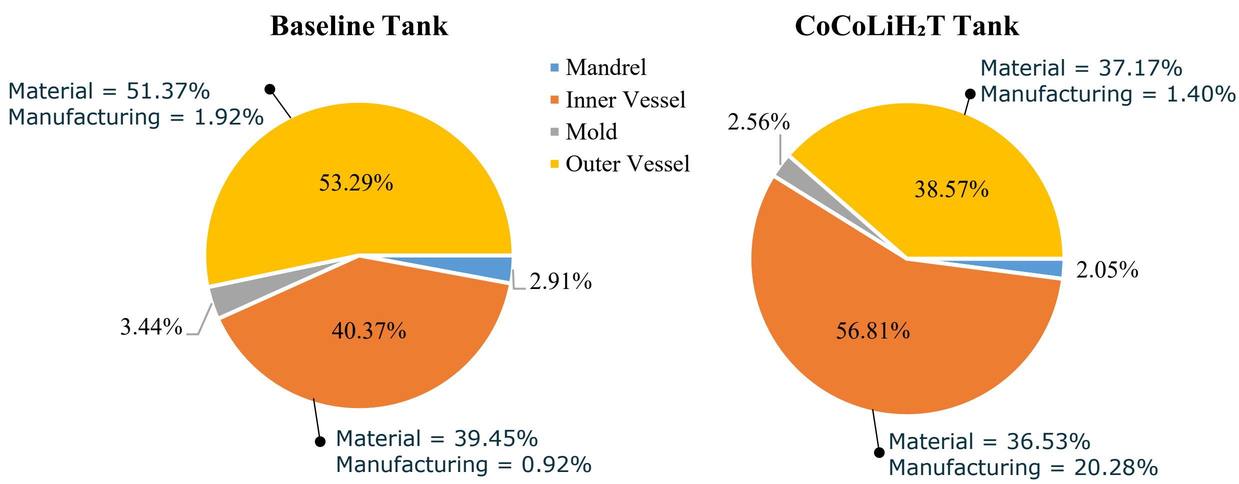

Figure 20 Average percentage contributions of each tank component towards environmental impact

Another interesting observation from the results was that the mandrel and mold contribute disproportionately towards *human carcinogenic toxicity* and *land use*, respectively. Their contribution pattern differ noticeably from the average values, as illustrated in Figure 21.

In the case of *human carcinogenic toxicity*, the mandrel emerges as the dominant contributor, accounting for approximately 45% of the total impact in both EoL scenarios. This contribution is primarily attributed to the landfilling of slag generated during steel production via the electric arc furnace route. Conversely, in the *land use* category, the mold is though not biggest, but an eminent contributor, responsible for approximately 23% of the total impact in both EoL scenarios. This result is driven by land occupation associated with forestry activities for wood production used to manufacture MDF. In this category, the mandrel contribution is negligible and effectively invisible in the contribution breakdown. Importantly, the relative distribution across components remains similar between the two EoL scenarios, indicating that these effects are driven mainly by material production rather than EoL treatment.

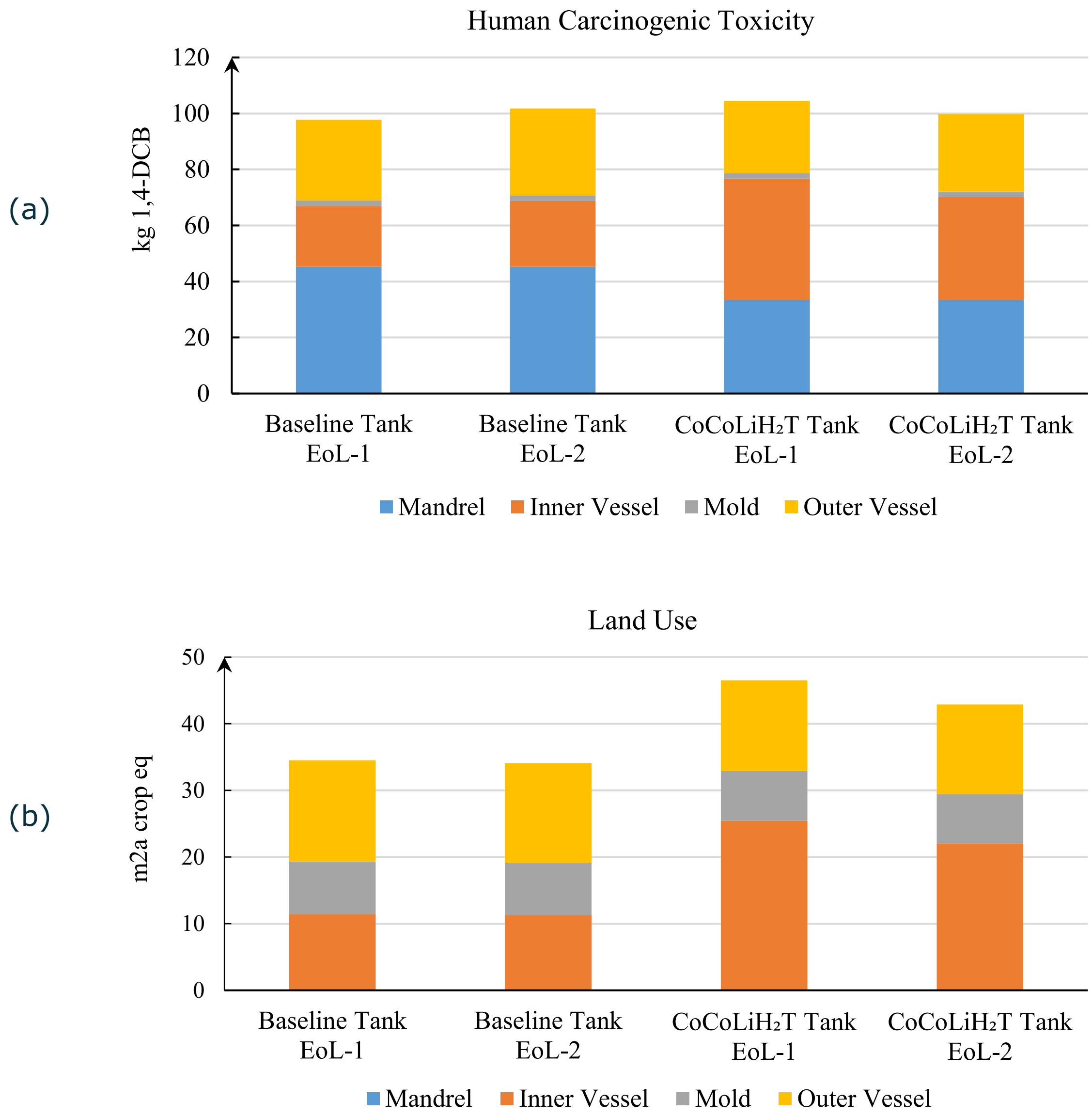

Figure 21 Comparison of contribution of each component of the tank towards the emissions related to (a) human carcinogenic toxicity and (b) land use

9.5.2 COCOLIH2T tank

For the COCOLIH2T tank, on average, the combined contribution of the mandrel and mold remains below 5% across both EoL scenarios (Figure 20), consistent with the trends observed for the baseline tank. However, the distribution between the inner and outer vessels differs substantially and contrarily, in this case, the inner vessel is found to be the dominant contributor to environmental impacts.

Under EoL Scenario-1, the inner vessel accounts for approximately 59% of total emissions, while the outer vessel contributes about 36%. Under EoL Scenario-2, the contribution of the inner vessel decreases slightly to ~54%, with a corresponding increase in the outer vessel contribution to ~41%. Average contributions across all categories and EoL scenarios for the tank are presented in Figure 20. As with the baseline tank, most impact categories show deviations of no more than ±5% from these average values. As shown in the figure, higher contribution of the inner vessel here can be attributed to the high energy consumption during AFP manufacturing, which contributed more than 20% of total emissions on average. Even when the inner vessel of the COCOLIH2T tank is approximately 1.6 times heavier than that of baseline tank, their relative contribution towards the total environmental impact of each tank is rather similar, when contributions only from the material usage are being considered. This highlights the benefits of using thermoplastics in the design, which is able to offset the increased impacts associated with the extra material consumption.

Once again, as shown in Figure 21, *human carcinogenic toxicity* and *land use* stand out as exceptions. For the same reasons discussed earlier, the mandrel contributes disproportionately to the former category, while the mold contributes significantly to the latter, despite their impacts being distributed over multiple production cycles. This consistency across tank designs reinforces the conclusion that these impact categories are strongly influenced by the production of the mandrel and the mold, rather than by tank architecture or EoL strategy.

9.6 Closure

The cradle-to-grave analysis of both tank designs indicates that the COCOLIH2T tank exhibits higher environmental burdens than the baseline tank in general. Under the EoL scenario of incineration and recycling, the performance gap between the two designs is narrower compared to when landfilling is considered as EoL pathway. However, the COCOLIH2T tank still shows higher impacts in nearly all categories, with one exception.

Normalization using global per-capita averages highlights that for the most influential impact categories, the normalized impact scores of the two tanks are comparable under the incineration and recycling EoL scenario, suggesting that the COCOLIH2T tank could achieve equivalent environmental performance to the baseline design when supported by improved EoL strategies.

10 Conclusions and Discussion

The life cycle assessment study for the COCOLIH2T project provides a comprehensive comparison between a novel conformal thermoplastic liquid hydrogen tank and a conventional cylindrical thermoset baseline tank. Evaluated across eighteen environmental impact categories and two distinct end-of-life (EoL) scenarios, the study highlights critical trade-offs between design innovation and environmental sustainability.

At a material level, thermoplastic composites demonstrate a clear environmental advantage over traditional thermoset systems, particularly when recycling is employed for the thermoplastics. However, despite the benefits of the material system, the current cradle-to-grave analysis reveals that the COCOLIH2T tank exhibits a higher overall environmental footprint than the baseline tank in almost all categories. This outcome is primarily driven by two factors, (i) increased mass requirement of the conformal inner vessel, approximately 1.6 times heavier than the baseline to compensate for less favourable stress distributions, and (ii) the high energy intensity of Automated Fibre Placement (AFP) manufacturing, which is approximately 24 times more energy-demanding per kilogram of material than the filament winding process used for the baseline vessel.

Considering the different EoL scenarios, under Scenario-2 (incineration and recycling), the environmental credits gained from recycling the CF/PAEK inner vessel significantly narrow the performance gap between the two tanks. Normalization of results against global per capita averages reveals that the most influential impact categories show a comparable performance between the two tank designs when a EoL strategy of incineration and recycling is utilised. Moreover, the critical analysis of these categories highlighted that the use of renewable energy resources as well as developing better tools for plastic recycling can further enhance the sustainability of the hydrogen storage system.

The study also underscores how modelling assumptions can significantly influence LCA results. In laboratory-scale assessments where impacts related to mandrel and molds are attributed to a single unit, the COCOLIH2T tank appears superior in several categories. However, in an industrial-scale production where impacts of mandrel and molds are distributed over 100 cycles, the environmental burden shifts almost entirely to the vessels themselves.

In conclusion, while challenges remain, the COCOLIH2T tank demonstrates long-term circularity potential and provides a viable pathway for sustainable liquid hydrogen storage in future aircraft.

11 References (Part – II)

[1] Golui DK. Environmental impact of aviation industry. Thiruvananthapuram, India: Environmental Science and Engineering Report, IIST 2020.

[2] Rupcic L, Pierrat E, Saavedra-Rubio K, Thonemann N, Ogugua C, Laurent A. Environmental impacts in the civil aviation sector: Current state and guidance. Transp Res D Transp Environ 2023;119. https://doi.org/10.1016/j.trd.2023.103717.

[3] Dincer I, Acar C. A review on potential use of hydrogen in aviation applications. vol. X, No. Y. n.d.

[4] Verstraete D. Long range transport aircraft using hydrogen fuel. Int J Hydrogen Energy 2013;38:14824–31. https://doi.org/10.1016/j.ijhydene.2013.09.021.

[5] Janić M. Greening commercial air transportation by using liquid hydrogen (LH2) as a fuel. Int. J. Hydrogen Energy, vol. 39, Elsevier Ltd; 2014, p. 16426–41. https://doi.org/10.1016/j.ijhydene.2014.08.011.

[6] Nojoumi H, Dincer I, Naterer GF. Greenhouse gas emissions assessment of hydrogen and kerosene-fueled aircraft propulsion. Int J Hydrogen Energy 2009;34:1363–9. https://doi.org/10.1016/j.ijhydene.2008.11.017.

[7] Bicer Y, Dincer I. Life cycle evaluation of hydrogen and other potential fuels for aircrafts. Int J Hydrogen Energy 2017;42:10722–38. https://doi.org/10.1016/j.ijhydene.2016.12.119.

[8] Pereira SR, Fontes T, Coelho MC. Can hydrogen or natural gas be alternatives for aviation? - A life cycle assessment. Int. J. Hydrogen Energy, vol. 39, Elsevier Ltd; 2014, p. 13266–75. https://doi.org/10.1016/j.ijhydene.2014.06.146.

[9] Khandelwal B, Karakurt A, Sekaran PR, Sethi V, Singh R. Hydrogen powered aircraft: The future of air transport. Progress in Aerospace Sciences 2013;60:45–59. https://doi.org/10.1016/j.paerosci.2012.12.002.

[10] Usman MR. Hydrogen storage methods: Review and current status. Renewable and Sustainable Energy Reviews 2022;167. https://doi.org/10.1016/j.rser.2022.112743.

[11] Niaz S, Manzoor T, Pandith AH. Hydrogen storage: Materials, methods and perspectives. Renewable and Sustainable Energy Reviews 2015;50:457–69. https://doi.org/10.1016/j.rser.2015.05.011.

[12] Kumar N, Lee SY, Park SJ. Advancements in hydrogen storage technologies: A comprehensive review of materials, methods, and economic policy. Nano Today 2024;56. https://doi.org/10.1016/j.nantod.2024.102302.

[13] Bosu S, Rajamohan N. Recent advancements in hydrogen storage - Comparative review on methods, operating conditions and challenges. Int J Hydrogen Energy 2024;52:352–70. https://doi.org/10.1016/j.ijhydene.2023.01.344.

[14] Yang M, Hunger R, Berrettoni S, Sprecher B, Wang B. A review of hydrogen storage and transport technologies. Clean Energy 2023;7:190–216. https://doi.org/10.1093/ce/zkad021.

[15] Bouhala L, Karatrantos A, Reinhardt H, Schramm N, Akin B, Rauscher A, et al. Advancement in the Modeling and Design of Composite Pressure Vessels for Hydrogen Storage: A Comprehensive Review. Journal of Composites Science 2024;8. https://doi.org/10.3390/jcs8090339.

[16] Aziz M. Liquid hydrogen: A review on liquefaction, storage, transportation, and safety. Energies (Basel) 2021;14. https://doi.org/10.3390/en14185917.

[17] Naquash A, Agarwal N, Lee M. A Review on Liquid Hydrogen Storage: Current Status, Challenges and Future Directions. Sustainability (Switzerland) 2024;16. https://doi.org/10.3390/su16188270.

[18] Yan Y, Zhang J, Li G, Zhou W, Ni Z. Review on linerless type V cryo-compressed hydrogen storage vessels: Resin toughening and hydrogen-barrier properties control. Renewable and Sustainable Energy Reviews 2024;189. https://doi.org/10.1016/j.rser.2023.114009.

[19] Dewangan SK, Mohan M, Kumar V, Sharma A, Ahn B. A comprehensive review of the prospects for future hydrogen storage in materials-application and outstanding issues. Int J Energy Res 2022;46:16150–77. https://doi.org/10.1002/er.8322.

[20] Qiu Y, Yang H, Tong L, Wang L. Research progress of cryogenic materials for storage and transportation of liquid hydrogen. Metals (Basel) 2021;11. https://doi.org/10.3390/met11071101.

[21] The COCOLIH2T Project - COmposite COnformal LIquid H2 Tank n.d. https://www.cocolih2t.eu/ (accessed June 11, 2025).

[22] Ye L, Lu L. Environmental and economic evaluation of the high-pressured and cryogenic vessels for hydrogen storage on the sedan. International Journal of Low-Carbon Technologies 2023;18:144–9. https://doi.org/10.1093/ijlct/ctac126.

[23] Gerboni R, Demaio N, Maffia L, Rossi S. LCA of a carbon fibre wrapped pressure vessel for automotive applications. 6th International Conference on EcoBalance-EcoBalance2004-25-27 October, 2004.

[24] Agostini A, Belmonte N, Masala A, Hu J, Rizzi P, Fichtner M, et al. Role of hydrogen tanks in the life cycle assessment of fuel cell-based auxiliary power units. Appl Energy 2018;215:1–12. https://doi.org/10.1016/j.apenergy.2018.01.095.

[25] Neelis ML, Van der Kooi HJ, Geerlings JJC. Exergetic life cycle analysis of hydrogen production and storage systems for automotive applications. Int J Hydrogen Energy 2004;29:537–45. https://doi.org/10.1016/S0360-3199(03)00087-9.

[26] Benitez A, Wulf C, de Palmenaer A, Lengersdorf M, Röding T, Grube T, et al. Ecological assessment of fuel cell electric vehicles with special focus on type IV carbon fiber hydrogen tank. J Clean Prod 2021;278. https://doi.org/10.1016/j.jclepro.2020.123277.

[27] Evangelisti S, Tagliaferri C, Brett DJL, Lettieri P. Life cycle assessment of a polymer electrolyte membrane fuel cell system for passenger vehicles. J Clean Prod 2017;142:4339–55. https://doi.org/10.1016/j.jclepro.2016.11.159.

[28] Dai Q, Lastoskie CM. Life cycle assessment of natural gas-powered personal mobility options. Energy and Fuels 2014;28:5988–97. https://doi.org/10.1021/ef5009874.

[29] Bionaz D, Marocco P, Ferrero D, Sundseth K, Santarelli M. Life cycle environmental analysis of a hydrogen-based energy storage system for remote applications. Energy Reports 2022;8:5080–92. https://doi.org/10.1016/j.egyr.2022.03.181.

[30] Sarkar A, Banerjee R. Net energy analysis of hydrogen storage options. Int J Hydrogen Energy 2005;30:867–77. https://doi.org/10.1016/j.ijhydene.2004.10.021.

[31] Weiszflog E, Abbas M. Life Cycle Assessment of Hydrogen Storage Systems for Trucks An assessment of environmental impacts and recycling flows of carbon fiber 2022.

[32] ecoinvent Version 3.8 n.d. https://support.ecoinvent.org/ecoinvent-version-3.8 (accessed June 11, 2025).

[33] Database - ecoinvent n.d. https://ecoinvent.org/database/ (accessed June 11, 2025).

[34] System Models n.d. https://support.ecoinvent.org/system-models (accessed June 11, 2025).

[35] Handbook I. Analysis of existing environmental impact assessment methodologies for use in life cycle assessment. Joint Research Center-European Commission 2010.

[36] Hauschild MZ, Rosenbaum RK, Olsen SI. Life Cycle Assessment. Cham: Springer International Publishing; 2018. https://doi.org/10.1007/978-3-319-56475-3.

[37] Ciroth A, Arvidsson R. Life Cycle Inventory Analysis: Methods and Data. Springer International Publishing; 2021.

[38] Huijbregts MAJ, Steinmann ZJN, Elshout PMF, Stam G, Verones F, Vieira M, et al. ReCiPe2016: a harmonised life cycle impact assessment method at midpoint and endpoint level. International Journal of Life Cycle Assessment 2017;22:138–47. https://doi.org/10.1007/s11367-016-1246-y.

[39] ReCiPe R. ReCiPe 2016 A harmonized life cycle impact assessment method at midpoint and endpoint level Report I: Characterization. 2016.

[40] ReCiPe R. ReCiPe 2016 v1.1 A harmonized life cycle impact assessment method at midpoint and endpoint level Report I: Characterization. 2017.

[41] Suzuki T, Takahashi J. Prediction of energy intensity of carbon fiber reinforced plastics for mass-produced passenger cars. Proceedings of 9th Japan international SAMPE symposium, Department of Environmental and Ocean Engineering, The University of Tokyo Japan; 2005, p. 14–9.

[42] Arblaster T. Environmental trade-offs of aerostructures: A prospective lifecycle assessment of wing ribs. 2023.

[43] Borda F, Ingarao G, Ambrogio G, Gagliardi F. Cumulative energy demand analysis in the current manufacturing and end-of-life strategies for a polymeric composite at different fibre-matrix combinations. J Clean Prod 2024;449:141775.

[44] Ogugua CJ, Anton S V, Tripathi AP, Larrabeiti MD, van Hees SO, Sinke J, et al. Energy analysis of autoclave CFRP manufacturing using thermodynamics based models. Compos Part A Appl Sci Manuf 2023;166:107365.

[45] Baley C, Davies P, Troalen W, Chamley A, Dinham-Price I, Marchandise A, et al. Sustainable polymer composite marine structures: Developments and challenges. Prog Mater Sci 2024;145:101307. https://doi.org/10.1016/j.pmatsci.2024.101307.

[46] Liddell H, Dollinger C, Fisher A, Brueske S, Cresko J. Bandwidth study on energy use and potential energy saving opportunities in US Carbon Fiber Reinforced Polymer Manufacturing. Report Number: DOE/EE-1662 2017.

[47] Cheng H, Guo L, Zheng L, Qian Z, Su S. A closed-loop recycling process for carbon fiber-reinforced polymer waste using thermally activated oxide semiconductors: Carbon fiber recycling, characterization and life cycle assessment. Waste Management 2022;153:283–92. https://doi.org/10.1016/j.wasman.2022.09.008.

[48] Gopalraj SK, Deviatkin I, Horttanainen M, Kärki T. Life cycle assessment of a thermal recycling process as an alternative to existing cfrp and gfrp composite wastes management options. Polymers (Basel) 2021;13. https://doi.org/10.3390/polym13244430.

[49] Kočí V, Picková E. Life cycle perspective of liquid epoxy resin use in the automotive industry. Pol J Environ Stud 2020;29:653–67. https://doi.org/10.15244/pjoes/100495.

[50] Witik RA, Teuscher R, Michaud V, Ludwig C, Månson JAE. Carbon fibre reinforced composite waste: An environmental assessment of recycling, energy recovery and landfilling. Compos Part A Appl Sci Manuf 2013;49:89–99. https://doi.org/10.1016/j.compositesa.2013.02.009.

[51] Pillain B, Loubet P, Pestalozzi F, Woidasky J, Erriguible A, Aymonier C, et al. Positioning supercritical solvolysis among innovative recycling and current waste management scenarios for carbon fiber reinforced plastics thanks to comparative life cycle assessment. Journal of Supercritical Fluids 2019;154. https://doi.org/10.1016/j.supflu.2019.104607.